

Flow-mediated effects on travel time, routing, and survival of juvenile Chinook salmon in a spatially complex, tidally forced river delta

Russell W. Perry, Adam C. Pope, Jason G. Romine, Patricia L. Brandes, Jon R. Burau, Aaron R. Blake, Arnold J. Ammann, and Cyril J. Michel

Abstract: We evaluated the interacting influences of river flows and tides on travel time, routing, and survival of juvenile late-fall Chinook salmon (*Oncorhynchus tshawytscha*) migrating through the Sacramento–San Joaquin River Delta. To quantify these effects, we jointly modeled the travel time, survival, and migration routing in relation to individual time-varying covariates of acoustic-tagged salmon within a Bayesian framework. We used observed arrival times for detected individuals and imputed arrival times for undetected individuals to assign covariate values in each reach. **We found travel time was inversely related to river inflow in all reaches, yet survival was positively related to inflow only in reaches that transitioned from bidirectional tidal flows to unidirectional flow with increasing inflows.** We also found that **the probability of fish entering the interior Delta, a low-survival reach, declined as inflow increased.** Our study illustrates how river inflows interact with tides to influence fish survival during the critical transition between freshwater and ocean environments. Furthermore, our analytical framework introduces new techniques to integrate formally over missing covariate values to quantify effects of time-varying covariates.

Résumé : Nous avons évalué l'interaction des influences des débits de rivière et des marées sur le temps de déplacement, l'itinéraire et la survie de saumons quinnats (*Oncorhynchus tshawytscha*) juvéniles de fin d'automne migrant dans le delta des fleuves Sacramento et San Joaquin. Pour quantifier ces effets, nous avons modélisé conjointement le temps de déplacement, la survie et l'itinéraire de migration par rapport à différentes covariables variant dans le temps de saumons dotés d'étiquettes acoustiques dans un cadre bayésien. Nous avons utilisé les temps d'arrivée observés pour les individus détectés et imputés des temps d'arrivée pour les individus non détectés afin d'affecter des valeurs aux covariables dans chaque tronçon. Nous constatons que le temps de déplacement est inversement relié au débit entrant dans tous les tronçons, alors que la survie n'est positivement reliée au débit entrant que dans les tronçons où des débits tidaux bidirectionnels passent à un écoulement unidirectionnel quand les débits entrants augmentent. Nous constatons aussi que la probabilité que les poissons entrent dans le delta intérieur, un tronçon caractérisé par une faible survie, diminue quand le débit entrant augmente. L'étude illustre comment les débits entrants de rivières interagissent avec les marées pour influencer la survie des poissons durant le passage critique du milieu d'eau douce au milieu océanique. En outre, notre cadre d'analyse présente de nouvelles méthodes permettant l'intégration formelle sur des valeurs de covariables manquantes pour quantifier les effets de covariables variant dans le temps. [Traduit par la Rédaction]

Introduction

Anadromous salmonids have evolved diverse life history strategies that capitalize on spatial and temporal variation in their habitat to maximize productivity. Understanding how salmonids use habitat over space and time can provide insight into population dynamics and help to identify particularly sensitive stages in their life history. Regulated rivers influence migrations of anadromous salmonids by altering the timing, magnitude, variation, and constituents of river discharge (e.g., temperature, turbidity), which in turn can affect their survival (Raymond 1988; Smith et al. 2003). Thus, interest often centers on how regulation of river flow affects survival of juvenile salmonids at different locations and times (Skalski et al. 2002; Michel et al. 2015).

Juvenile Chinook salmon (*Oncorhynchus tshawytscha*) in the Central Valley of California, USA, emigrate from natal tributaries of

the Sacramento River through the Sacramento–San Joaquin River Delta (henceforth, “the Delta”), a network of natural and man-made channels linking the Sacramento and San Joaquin rivers to San Francisco Bay and the Pacific Ocean (Fig. 1). The Delta is the hub of California's water delivery system, providing agricultural and domestic water that supports California's economy, the eighth largest in the world (Healey et al. 2016). Water from the Sacramento River is diverted from the north through natural channels and gated man-made channels to the south where large pumping stations “export” water from the Delta in canals (Fig. 1). As juvenile salmon enter the Delta, they distribute among its complex channel network where they are subject to channel-specific abiotic and biotic factors that influence their migration timing, growth, and survival. For example, fish that enter the interior Delta, the region to the south of the mainstem Sacra-

Received 27 July 2017. Accepted 17 December 2017.

R.W. Perry, A.C. Pope, and J.G. Romine.* US Geological Survey, Western Fisheries Research Center, 5501A Cook-Underwood Road, Cook, WA 98605, USA.

P.L. Brandes. US Fish and Wildlife Service, 850 Guild Ave., Suite 105, Lodi, CA 95240, USA.

J.R. Burau and A.R. Blake. US Geological Survey, California Water Science Center, 6000 J Street, Placer Hall, Sacramento, CA 95819, USA.

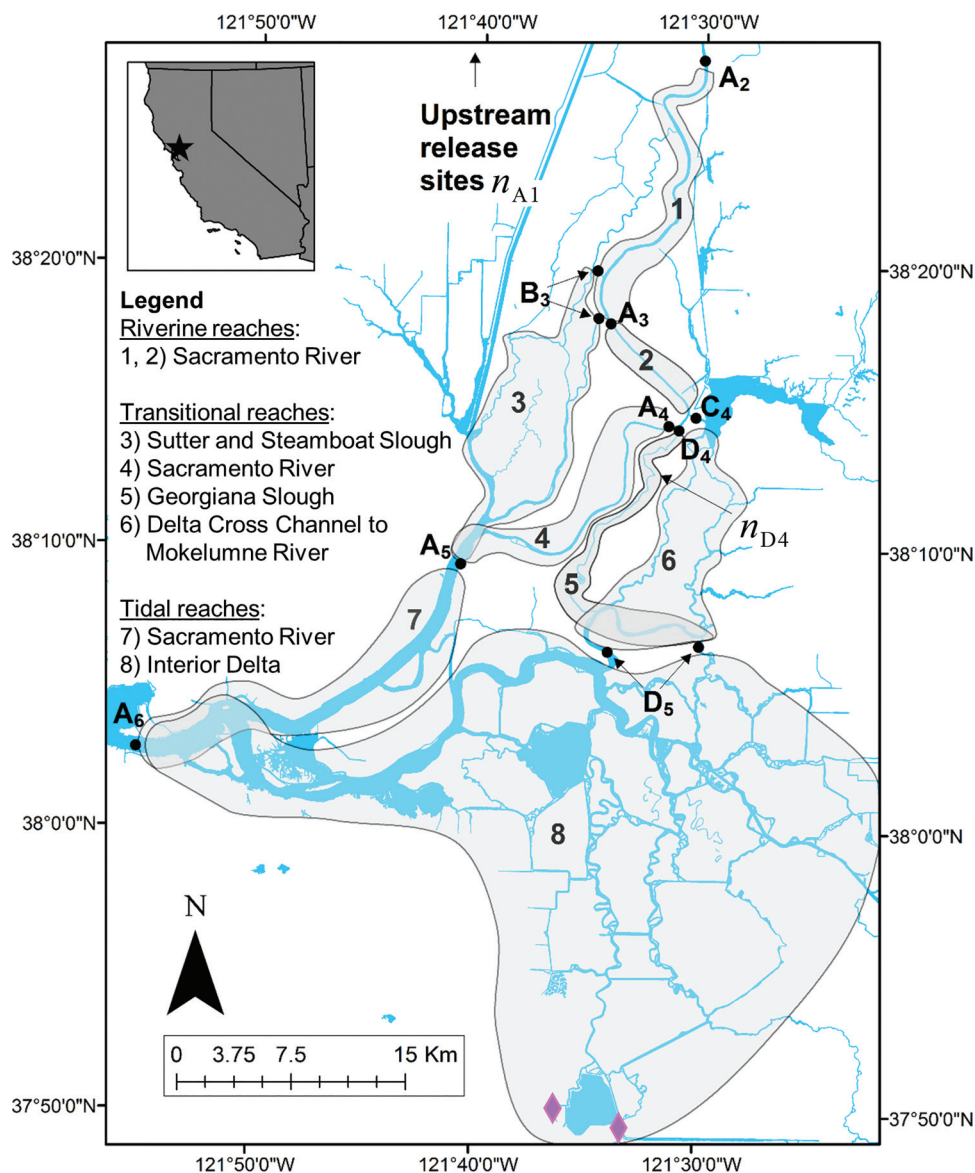
A.J. Ammann and C.J. Michel. National Marine Fisheries Service, Southwest Fisheries Science Center, 110 Shaffer Rd., Santa Cruz, CA 95060, USA.

Corresponding author: Russell W. Perry (email: rperry@usgs.gov).

*Present address: US Fish and Wildlife Service, Mid-Columbia River National Wildlife Refuge Complex, 64 Maple St., Burbank, WA 99323, USA.

Copyright remains with the author(s) or their institution(s). Permission for reuse (free in most cases) can be obtained from [RightsLink](https://www.elsevier.com/locate/permissions).

Fig. 1. Map of the Sacramento–San Joaquin River Delta showing the location of acoustic telemetry receiving stations (filled black circles) used to detect acoustic tagged juvenile salmon as they migrated through the Delta. Telemetry stations are labeled by migration route (A–D) and sampling occasion (1–7; see Fig. 2). These telemetry stations divide the Delta into eight discrete reaches (shown by numbered shaded regions), with an additional reach upstream of telemetry station A_2 (reach 0) used as acclimation reach to allow fish to recover from postrelease handling. The location of water pumping stations in the southern interior Delta is indicated by the diamonds at the bottom. Data and maps copyright © 1999–2006 ESRI.



mento River (reach 8 in Fig. 1), survive at lower rates than fish migrating through northerly routes, likely owing to longer travel times, longer travel distances, higher predation rates, and entrainment at the pumping stations (Brandes and McLain 2001; Newman and Brandes 2010; Perry et al. 2010, 2013).

Survival of juvenile salmon has been positively related to river discharge at the Delta-wide scale (Kjelson et al. 1982; Kjelson and Brandes 1989; Newman and Rice 2002; Newman 2003), but the underlying factors driving this relationship remain unclear. Low river discharge has been associated with a high proportion of fish entering the interior Delta, thereby decreasing overall survival by subjecting a larger fraction of the population to low survival probabilities (Perry et al. 2015). What remains unclear is the extent to which within-reach survival contributes to the overall flow–survival relationship. Is survival related to discharge in all reaches, or do a few key reaches drive the overall flow–survival relationship?

Given that the Delta transitions from unidirectional flow in its upper reaches to tidally driven bidirectional flows in lower reaches, we hypothesized that the reach-specific relationship between inflow and survival could vary along this gradient. Understanding exactly which reaches contribute to the overall flow–survival relation will help researchers to focus on specific mechanisms driving this relationship and help managers to target specific actions to increase survival.

Here, we analyze acoustic telemetry data on juvenile Chinook salmon from 17 distinct release groups collected from two studies conducted between 2007 and 2011 (Table 1) to understand how reach-specific travel time, migration routing, and survival vary among reaches in the Sacramento–San Joaquin River Delta. Because each release group spreads out over time as they migrated through the Delta, individuals entered a given reach over a wide range of environmental conditions. Our interest therefore cen-

Table 1. Description of release groups and data sources.

Release group	Source	Year	Release dates	No. released	No. analyzed	Release sites (rkm)
1	Perry et al. 2010, 2013	2006	5–6 Dec.	64	64	172
2	Perry et al. 2010, 2013	2007	17–18 Jan.	80	80	172
3	Michel et al. 2015		15 Jan. – 2 Feb.	200	11	517
4	Perry et al. 2013		4–7 Dec.	208	208	115, 172
5	Michel et al. 2015		7 Dec.	150	60	345, 398, 500
6	Perry et al. 2013	2008	15–18 Jan.	211	211	115, 172
7	Michel et al. 2015		17 Jan.	154	65	345, 398, 500
8	Perry et al. 2013		30 Nov. – 6 Dec.	292	292	115, 172
9	Michel et al. 2015		13 Dec.	149	82	345, 398, 500
10	Michel et al. 2015	2009	11 Jan.	151	63	345, 398, 500
11	Perry et al. 2013		13–19 Jan.	292	292	115, 172
12	Perry et al. 2012		2–5 Dec.	239	239	115, 191
13	Michel et al. 2015		15 Dec.	153	63	345, 398, 500
14	Perry et al. 2012		16–19 Dec.	240	240	115, 191
15	Michel et al. 2015	2010	6 Jan.	153	42	345, 398, 500
16	Michel et al. 2015		17 Dec.	120	79	500
17	Michel et al. 2015	2011	5 Jan.	120	79	500
All groups				2976	2170	

Note: Release sites are indicated by river kilometre (rkm) measured from the distance to the Pacific Ocean. For fish released upstream of the Delta (>rkm 208), the number analyzed indicates fish that were included in the analysis based on detections at telemetry stations near the entrance to the Delta at rkm 189 or rkm 226.

tered on quantifying factors affecting individual variation in survival. However, time-varying individual covariates are a vexing problem in conventional mark–recapture models (e.g., maximum likelihood estimation performed in Program Mark; White and Burnham 1999) because the value of the covariate is unknown when an individual is undetected, rendering the likelihood analytically intractable in most cases (but see Catchpole et al. 2008). Therefore, we developed a Bayesian hierarchical model that jointly modeled both travel times and survival of juvenile salmon. The travel time model was used to impute arrival times of undetected fish in each reach, which allowed us to define covariate values based on imputed arrival times for undetected individuals. We then used Markov chain Monte Carlo (MCMC) techniques to integrate the likelihood over the missing covariate values while simultaneously estimating parameters associated with both travel time and survival.

Methods

Study area and telemetry system

The telemetry system was designed to accommodate requirements of a multistate mark–recapture model that estimated reach- and route-specific survival for nine discrete reaches and four primary migration routes through the Delta (Perry et al. 2010; Figs. 1 and 2). The nine reaches separate the Delta into the three hydrodynamic zones: (i) riverine reaches with unidirectional flows and the least influence of tidal forcing (reaches 0–2), (ii) transitional reaches that shift from unidirectional flow to tidally driven bidirectional flows as river flow entering the Delta decreases (reaches 3–6), and (iii) tidal reaches with bidirectional flows regardless of the amount of river flow entering the Delta (reaches 7–8; Figs. 1 and 3). These nine reaches comprise four distinct migration routes that constitute the states of the multistate model: the Sacramento River (Route A = reaches 1, 2, 4, and 7), Sutter and Steamboat Slough (Route B = reaches 1, 3, and 7), the Delta Cross Channel (Route C = reaches 1, 2, 6, and 8), and Georgiana Slough (Route D = reaches 1, 2, 5, and 8; Figs. 1 and 2).

Each telemetry station consisted of single or multiple tag-detecting monitors (Vemco Model VR2, Amirix Systems, Inc., Halifax, Nova Scotia, Canada), depending on the number of monitors needed to maximize detection probabilities at each station. Migration routes A, B, C, and D were monitored with 7, 1, 1, and 2 telemetry stations, respectively, labeled according to migration

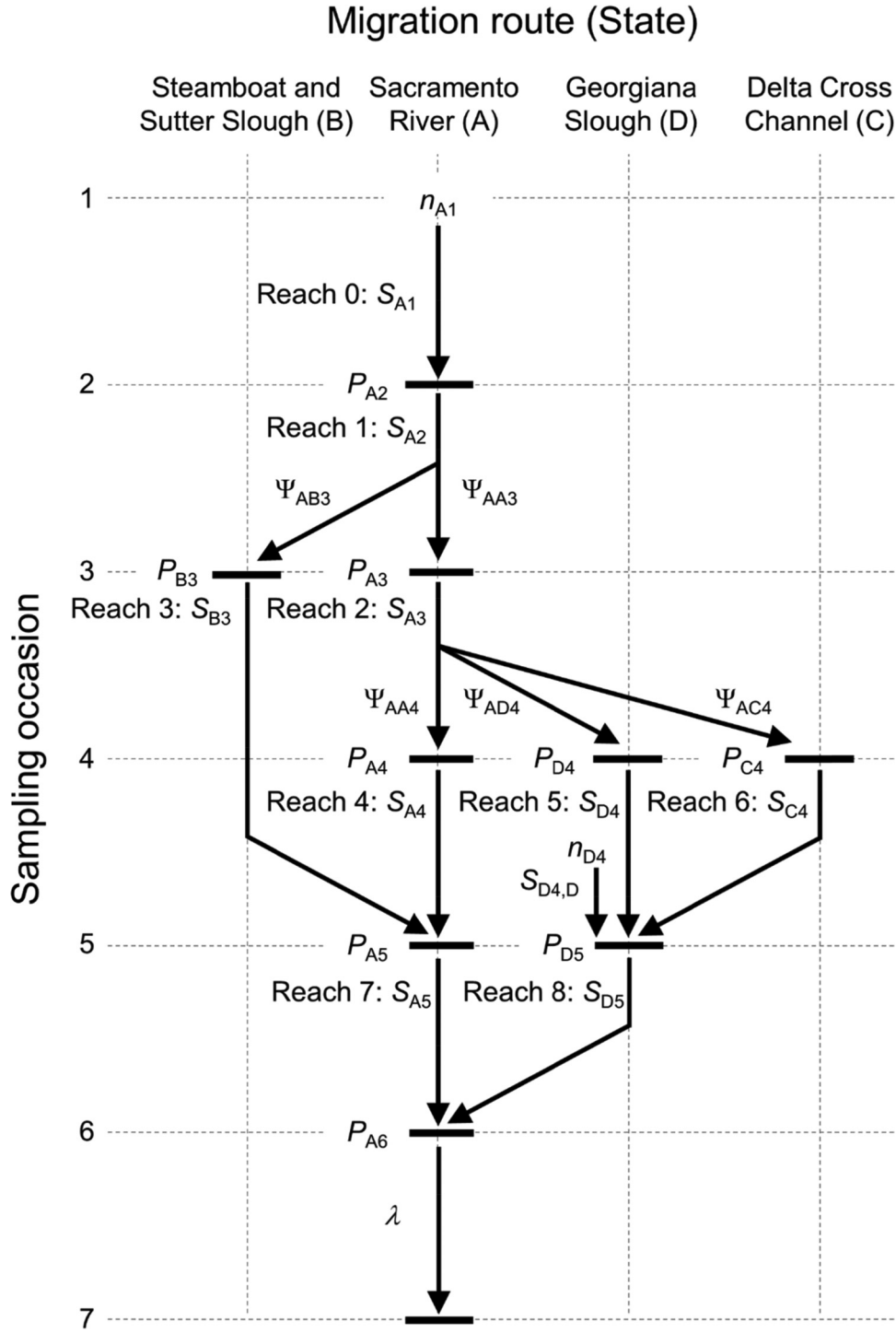
route r at sampling occasion j (Figs. 1 and 2). Sampling occasion was defined based on the j th telemetry station within the mainstem Sacramento River, with the upstream release site defined as occasion one. Migrating juvenile salmon first arrive at Sutter and Steamboat Slough (B_3), which diverges from the Sacramento River at the first river junction and converges again with the Sacramento River upstream of A_5 (Figs. 1 and 2). Fish remaining in the Sacramento River then pass the Delta Cross Channel (C_4), a man-made gated canal that diverts fish, when its gates are open, into reach 6 and subsequently into the interior Delta (reach 8). The Delta Cross Channel is used to control salinity at the water pumping stations, undergoes mandatory closures for fisheries protection in mid-December each year, and also closes when Sacramento River flow exceeds $708 \text{ m}^3 \cdot \text{s}^{-1}$ ($25\,000 \text{ ft}^3 \cdot \text{s}^{-1}$). Fish then pass Georgiana Slough (D_4), a natural channel (reach 5) that also leads to the interior Delta (reach 8). All routes then converge at Chipps Island (A_6), the terminus of the Delta. With this configuration, survival to site A_6 is confounded with detection probability at the last telemetry station. Therefore, to estimate survival to A_6 , we pooled detections from numerous tag-detecting monitors downstream of A_6 in San Francisco Bay for estimating detection probability at Chipps Island.

Although there are numerous possible migration pathways, we focused on these four routes because management actions likely have the largest influence on movement and survival among these routes. For example, fish may enter the interior Delta from the Sacramento River through either Georgiana Slough or the Delta Cross Channel, where they subsequently become vulnerable to migration delays and entrainment at the water pumping projects (Perry et al. 2010; Newman and Brandes 2010). Sutter and Steamboat Slough is an important migration route because fish using this route bypass the Delta Cross Channel and Georgiana Slough (Fig. 1), thereby avoiding the interior Delta. Thus, monitoring these primary migration routes provides information about the likely ultimate fate of individuals.

Fish tagging and release

All juvenile late-fall Chinook salmon were obtained from the Coleman National Fish Hatchery in Anderson, California. Release groups were defined based on release timing and data source, with the exception of release group 3, which was pooled over a longer period of release times owing to small sample size (Table 1).

Fig. 2. Schematic of the multistate mark-recapture model with parameters indexed by state (migration route) and sampling occasion. Parameters include reach-specific survival probabilities (S), site-specific detection probabilities (P), routing probabilities (Ψ), and λ , the joint probability of surviving and being detected at telemetry stations downstream of site A_6 . Release locations are indicated by the n th release in route r at occasion j : n_{A1} (at Sacramento or upstream — see Table 1) and n_{D4} in Georgiana Slough.

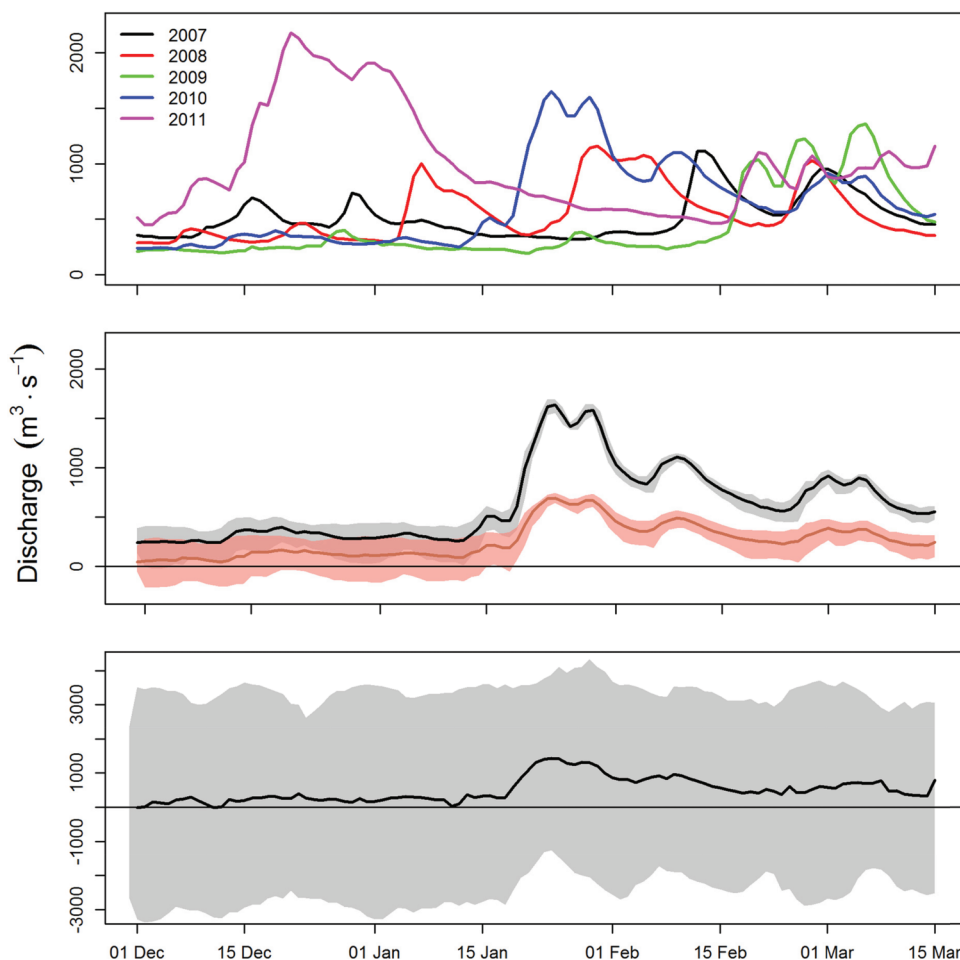


All fish other than release group 1 were tagged with a 69 kHz acoustic tag weighing 1.58 g (Vemco Model V7-2L-R64K, Amirix Systems, Inc., Halifax, Nova Scotia, Canada) transmitting either every 30–90 s (release groups 1–3) or 15–60 s (release groups 4–17). Battery life of these transmitters ranged from 98 to 749 days based on tests conducted by Michel et al. (2015). Fish from release group 1 were tagged with an acoustic tag weighing 1.44 g, which had an expected battery life of 70 days (Vemco Model V7-2L-R64K).

Most juvenile salmon were surgically tagged at the hatchery and then transported to release sites, but fish from release groups 8 and 11 were tagged at release sites. Fish were randomly selected, and those ≥ 140 mm fork length were retained for tagging to maintain tag burden below 6% of the fish mass. Fish tagged by Michel et al. (2015) were held at the hatchery for 24 h following surgery, transported to release sites, and held in-river for 1–3 h prior to release. Fish tagged by Perry et al. (2010, 2012, 2013) were trans-

Can. J. Fish. Aquat. Sci. Downloaded from www.nrcresearchpress.com by CA DEPARTMENT OF FISH AND WILDLIFE on 08/02/19
For personal use only.

Fig. 3. Daily inflow into the Sacramento–San Joaquin River Delta (top panel) and tidal influence on discharge at three locations in the Sacramento River during 2010 (middle and bottom panels). The top panel shows mean daily discharge of the Sacramento River at Freeport (A_2 in Fig. 1). In the two lower panels, lines show mean daily discharge, and the shaded regions encompass the daily minimum and maximum discharge, with values <0 indicating reverse flows caused by tidal forcing. The middle panel shows the Sacramento River at Freeport (black line, gray shading) and the Sacramento River just downstream of Georgiana Slough (pink line and shading; A_4 in Fig. 1). The bottom panel shows the Sacramento River at Rio Vista (A_5 in Fig. 1). [Colour online.]



ported to release sites, held in-river at release sites for 24 h, and then released into either the Sacramento River near Sacramento (n_{A1}) or Georgiana Slough (n_{D4} ; Fig. 1 and 2). Fish were released into Georgiana Slough to increase the number of fish entering the interior Delta (reach 8) and improve precision of survival estimates for that region. For the Michel et al. (2015) study, fish were released well upstream of the Delta, at four locations in the Sacramento River (Table 1). In most migration years, two releases were made: one in December and another in January. Releases in December occurred prior to seasonal closure of the Delta Cross Channel gates, which typically occurs on 15 December, whereas the Delta Cross Channel gates were closed for all January releases. Further details of tagging and release protocols can be found in the citations listed in Table 1.

Screening for false positive detections and predators

Telemetry data were screened for false positive detections by first summarizing data into detection events defined by the number of consecutive detections from an individual tag within a 30 min period at a given telemetry station. Any detection event with at least two detections at a given location was considered as valid. Detection events with a single detection were considered valid if the detection was consistent with the entire spatiotemporal detection history of the individual's tag (e.g., a single detection

was preceded by an upstream detection and proceeded by a downstream detection). Otherwise, single detections were considered false positives and removed from analysis.

Tags that may have been consumed by predators were identified by adapting the methods of Gibson et al. (2015), which consisted of several steps. First we calculated five movement metrics from tag detections that quantified differences in behavioral patterns between live tagged smolts and tagged smolts that had been consumed by predators such as striped bass (*Morone saxatilis*), smallmouth bass (*Micropterus dolomieu*), largemouth bass (*Micropterus salmoides*), and spotted bass (*Micropterus punctulatus*). The metrics included (i) the mean rate of downstream movement calculated as the shortest channel distance between consecutive detections of downstream movements divided by the elapsed time between detections, (ii) the number of consecutive detection events occurring at the same location, (iii) the cumulative distance travelled divided by the total number of days spent in the study area, (iv) the number of transitions between telemetry stations that were deemed to be only possible by a predator (i.e., movement upstream against the flow), and (v) the total time in the array from the time of release to the time of last detection.

Next we used hierarchical cluster analysis to group each tag by the multivariate characteristics of the five metrics. We used the

hclust package in R (R Core Team 2015) and divided the tags in three groups based on the dendrogram resulting from hierarchical clustering using Ward's minimum variance method (Ward 1963; Gibson et al. 2015). We then selected the group whose movement characteristics were most consistent with that of predator-like behavior (i.e., upstream movement against flow, long residence times near receivers, and low average distance travelled per day). We examined each tag's time series of movement metrics to identify if and when the tag transitioned from smolt-like to predator-like behavior. The detection history was then truncated at this point in the detection history. Overall, 17% percent of tags were flagged for review based on the movement metrics, and 11% percent exhibited predator-like behavior that required truncation of their capture history.

Structure of the mark-recapture model

The multistate mark-recapture model estimates three types of parameters from detections of acoustic-tagged juvenile Chinook salmon: $S_{r,j}$ is the probability of surviving from a telemetry station within route r at sampling occasion j to the next downstream telemetry station; $\Psi_{r,s,j}$ is the probability of entering route s from route r at sampling occasion j , conditional on surviving to occasion j (henceforth, routing probability); and $P_{r,j}$ is the probability of detecting a tagged fish at a telemetry station on sampling occasion j within route r , conditional on fish surviving to occasion j (Fig. 2). In the parlance of multistate mark-recapture models, the routes constitute the states, the routing probabilities represent the state transition probabilities, and survival and detection probabilities are conditioned on migration route (i.e., conditioned on state).

In addition, our modeling framework includes an auxiliary model for travel times, which we used to impute arrival times of undetected individuals in each reach for the purposes of assigning daily covariate values. This model estimates two travel time parameters associated with lognormally distributed travel times: $\mu_{r,j}$ is the mean of log-travel times from a telemetry station in route r at sampling occasion j to the next downstream telemetry station, and $\sigma_{r,j}^2$ is the variance of the travel times. Because reaches 1–8 are associated with a unique r, j combination (route, sampling occasion), we generally refer to travel time and survival parameters as being reach-specific (Figs. 1 and 2).

To understand how both migration routing and reach-specific survival contribute to overall survival through the Delta, we model the underlying parameters as functions of covariates and then reconstruct the overall relationship from these component parts. Overall survival through the Delta was reconstructed from the individual components as

$$(1) \quad S_{\text{Delta}} = \sum_{r \in \{A,B,C,D\}} \Psi_r S_r$$

where S_r is the survival from telemetry stations A_2 to A_6 (i.e., from the entrance to the exit of the Delta) for fish taking migration route r , and Ψ_r is the total probability of a fish taking route r . Thus, S_r is the product of reach-specific survival probabilities that trace a unique migration route through the Delta (e.g., $S_D = S_{A_2}S_{A_3}S_{D_4}S_{D_5}$), and Ψ_r is the product of routing probabilities along that route (e.g., $\Psi_D = \Psi_{AA_3}\Psi_{AD_4}$; Perry et al. 2010).

Time-varying individual covariates

We hypothesized that river discharge affected migration routing, travel times, survival, and detection probabilities. Mean daily discharge varies among the nine reaches owing to the distribution of total discharge among the Delta's channel network. However,

tidally averaged net discharge in most reaches is a direct function of (i) river flows entering the Delta (as measured in the Sacramento River at Freeport located near telemetry station A_2 in Fig. 1) and (ii) whether the Delta Cross Channel Gate is open or closed (Fig. S1; supplementary data are available online¹). Furthermore, as river inflow increases, tidal fluctuations are dampened in all but reaches 7 and 8 (Fig. 3). Therefore, we used river discharge at Freeport (Q) and the position of the Delta Cross Channel gate ($G = 1$ or 0 for gates open or gates closed, respectively) as an index of variation in reach-specific mean discharge affecting migration routing, travel times, survival, and detection probabilities. Specifically, time-varying individual covariates Q_d and G_d were assigned based on the day d when the i th individual passed a telemetry station in route r at sampling occasion j .

We modeled μ , the log-mean of the travel time distribution, as a linear function of individual time-varying covariates:

$$(2) \quad \mu_{i,r,j} = \alpha_{0,r,j} + \alpha_{1,r,j}Q_d + \alpha_{2,r,j}G_d + z_{\mu,n,r,j}\xi_{\mu,r,j}$$

where r, j indexes the route and occasion where individuals entered reaches 0, ..., 8 (Fig. 1 and 2), $\mu_{i,r,j}$ is the log-mean travel time for individual i in each reach, $\alpha_{0,r,j}$ is the intercept, $\alpha_{1,r,j}$ is the slope for the effect of discharge on μ , and $\alpha_{2,r,j}$ is the effect of Delta Cross Channel gate position on μ . We modeled $\sigma_{r,j}$, the variance parameter of the lognormal travel time distribution, as a constant for all individuals within a reach. In addition, $\alpha_{2,r,j}$ was set to zero for reaches located upstream of the Delta Cross Channel (i.e., for reaches 0, 1, 2, 3, and 6).

Given that discrete groups of fish were released in different months, years, and locations, we expected considerable variation in release-specific travel time, survival, and routing over and above variation that could be accounted for by covariates in the model. Extra variation among release groups was structured as a noncentered random effect, where $z_{\mu,n,r,j}$ in eq. 2 is a standard normal deviate for the n th release group entering each reach, $\xi_{\mu,r,j}$ is the standard deviation of the random effect in each reach, and their product is the deviation of each release group from the mean, conditional on the covariates. We used a noncentered random effect to reduce autocorrelation and speed convergence of the model fitting routine (Papaspiliopoulos et al. 2007; Monnahan et al. 2017).

Reach-specific survival was modeled as a logistic function using the same linear structure as travel time:

$$(3) \quad \text{logit}(S_{i,r,j}) = \beta_{0,r,j} + \beta_{1,r,j}Q_d + \beta_{2,r,j}G_d + \beta_3 l_i + z_{S,n,r,j}\xi_{S,r,j}$$

where $\text{logit}(\cdot)$ is the logit link function, l_i is the fork length of individual i , β_3 is the slope for the effect of fork length on survival, and all other coefficients are defined as in eq. 2 except with respect to survival. In this model, survival is constant among individuals that enter a given reach on a particular day. Travel time influences survival only through its effect on arrival times to a given telemetry station, which determines the discharge that individuals experienced when they entered a given reach.

We modeled three routing probabilities as a function of covariates: Ψ_{AB_3} , Ψ_{AC_4} , and $\Psi_{AD_4|C'}$. Here, Ψ_{AB_3} is the probability of entering Sutter and Steamboat Slough (route B) from the Sacramento River (route A) at sampling occasion 3, Ψ_{AC_4} is the probability of entering the Delta Cross Channel (route C) from the Sacramento River at sampling occasion 4, and $\Psi_{AD_4|C'}$ is the probability of entering Georgiana Slough (route D) from the Sacramento River, conditional on not having entered the Delta Cross Channel (C'). Since routing probabilities must sum to 1 at each of the two river

¹Supplementary data are available with the article through the journal Web site at <http://nrcresearchpress.com/doi/suppl/10.1139/cjfas-2017-0310>.

junctions, the unconditional probability of entering Georgiana Slough (Ψ_{AD4}) at sampling occasion 4 is $(1 - \Psi_{AC4})\Psi_{AD4|C}$.

We model routing probabilities using a generalized logistic function:

$$(4) \quad \Psi_i = L + \frac{U - L}{1 + \exp[-(\gamma_0 + \gamma_1 Q_d + \gamma_2 G_d + z_{\gamma,n} \xi_{\Psi})]}$$

where Ψ_i is one of the three routing probabilities described above for individual i , L is the lower limit of Ψ_i , U is the upper limit of Ψ_i , and all other parameters are described as in eq. 2 except with respect to routing. The parameters U and L allow the logistic function to take on values other than 1 or 0 for upper and lower limits, respectively. This equation reduces to the standard inverse logit function by setting $U = 1$ and $L = 0$. We used the generalized logistic function because we expected routing probabilities to follow a relationship similar to that between total discharge (Q) and the fraction of discharge entering each route. As these channels transition from bidirectional tidal flows to unidirectional flows with increasing total discharge, the fraction of discharge entering a route either increases (Sutter and Steamboat Slough) or decreases (Georgiana Slough) with discharge before leveling off at a constant fraction of discharge (Fig. S2¹). Therefore, for Sutter and Steamboat Slough (Ψ_{AB3}), we set $L = 0$ and $\gamma_2 = 0$; for the Delta Cross Channel (Ψ_{AC4}), we set $L = 0$, $U = 1$, and $\gamma_2 = 0$; and for Georgiana Slough ($\Psi_{AD4|C}$), we set $U = 1$.

We hypothesized that increases in discharge could reduce detection probabilities by increasing acoustic noise and by increasing the speed at which juvenile salmon pass telemetry stations. In addition, many telemetry stations were monitored each year with different hydrophones, varying numbers of hydrophones, and different spatial configurations that could have influenced detection probability. Therefore, we modeled these effects on detection probability as linear on the logit scale:

$$(5) \quad \text{logit}(P_{i,r,j}) = \theta_{0,r,j,y} + \theta_{1,r,j} Q_d$$

where $\theta_{0,r,j,y}$ is an intercept for year y at occasion j within route r , and $\theta_{1,r,j}$ is the slope for the effect of river discharge on detection probability at occasion j in route r .

Complete data likelihood

To estimate model parameters as a function of time-varying individual covariates, we used the complete data likelihood of the multistate model within a Bayesian framework. The complete data likelihood proceeds as if there were no missing values by augmenting the observed data with the unobserved missing data and treating the missing data as additional model parameters to be estimated (King et al. 2010; Link and Barker 2010). This approach relies on using an appropriate probability model for imputing missing covariate values and then constructing the joint likelihood of the mark-recapture model parameters, the covariate model parameters, and the missing data (Bonner and Schwarz 2004). To impute missing covariate values for nondetected individuals whose arrival times are unknown, we model arrival times by estimating parameters of the distribution of travel times through each reach.

The observed data for each individual required to estimate model parameters include (i) the detection history, (ii) cumulative travel times, (iii) reach-specific travel times, and (iv) covariates linked to the fish’s arrival time in each reach. A “detection history” is the alpha-numeric vector h_i indicating whether individual i was detected in route r at occasion j ($h_{i,j} = A, B, C,$ or D) or not detected at occasion j ($h_{i,j} = 0$). The detection history compactly represents each fish’s detection and movement history through the telemetry network. For example, the detection history A0ADD00 indicates a fish that was released into the Sacramento

River ($h_{i,1} = A$) and was not detected at A_2 but was detected at A_3 ($h_{i,2:3} = 0A$), indicating it remained in the Sacramento River at its junction with Sutter and Steamboat Slough. This fish was then detected entering Georgiana Slough at D_4 and once more at D_5 before never being detected again ($h_{i,4:7} = DD00$). Associated with the observed detection history of each individual is the vector of observed cumulative travel times T_i . For example, if $h_i = A0ADD00$ then $T_i = (T_{i,1}, NA, T_{i,3}, T_{i,4}, T_{i,5}, NA, NA)$ where $T_{i,1} = 0$, $T_{i,j}$ is the time from release to detection at a telemetry station at sampling occasion j , and $T_{i,j}$ is missing (NA) when an individual is not detected. Time-varying covariate values $x_{i,j}$ defined based on arrival date in each reach are missing (NA) whenever an individual is not detected. Thus, for A0ADD00, $x_i = (x_{i,1}, NA, x_{i,3}, x_{i,4}, x_{i,5}, NA, NA)$. Observed reach-specific travel times $t_{i,r,j}$ for individual i in route r at occasion j are obtained by taking the consecutive differences of the cumulative travel times. For A0ADD00, $t_i = (NA, NA, t_{i,A3}, t_{i,D4}, NA, NA)$. Note that $t_{i,r,j}$ is observed only when fish are detected at consecutive telemetry stations whereas $T_{i,j}$ is defined whenever a fish is detected.

Adapting the notation of King et al. (2010), the complete data likelihood augments the observed detection history, h_i , by imputing the latent (unobserved) states when individuals are not detected:

$$(6) \quad z_{i,j} = \begin{cases} h_{i,j} & \text{if } h_{i,j} \neq 0 \\ g_{i,j} & \text{if } h_{i,j} = 0 \end{cases}$$

where $g_{i,j}$ is the latent state of unobserved individual i at detection occasion j , $z_{i,j}$ is the state of individual i at detection occasion j (whether detected or nondetected), and z_i is the complete state history for individual i . Although death can never be directly observed in detection history h_i , death is included as a latent state such that $g_{i,j} \in (A, B, C, D, \dagger)$ where \dagger is the death state.

The complete data likelihood is the product of three conditional likelihoods: (i) a Bernoulli distribution for detection at occasion j given survival to occasion j in state r , (ii) a Bernoulli distribution for survival from occasion j to $j + 1$ in state r given survival to occasion j , and (iii) a generalized Bernoulli distribution (i.e., a multinomial distribution for a single observation) for the probability of moving from state r at occasion j to state s at occasion $j + 1$ given survival to occasion $j + 1$:

$$(7) \quad L[S, \Psi, P|h, g] = \prod_{i=1}^N \prod_{j=F_i}^{J-1} \prod_{r \in R_j} [P_{i,r,j+1}^{h_{i,j+1} + 1} (1 - P_{i,r,j+1})^{h_{i,j+1} - 1}] \times [S_{i,r,j}^{w_{i,j,r,\dagger}} (1 - S_{i,r,j})^{w_{i,j,r,\dagger} - 1}] \prod_{s \in R_{j+1}} \Psi_{i,r,s}^{w_{i,j,r,s}}$$

where F_i is the occasion of release for individual i ; R_j is the set of states, excluding the death state, available to an individual in state r at occasion j (Fig. 2); $u_{i,j,r} = I(h_{i,j} = r)$, and $I(\cdot)$ is an indicator function resolving to 1 if individual i is detected in state r at occasion j and 0 otherwise; $v_{i,j,r} = I(g_{i,j} = r)$ is 1 if individual i is imputed to be in state r at detection occasion j and 0 otherwise; $w_{i,j,r,s} = I(z_{i,j} = r, z_{i,j+1} = s)$ is 1 if individual i is in state r at detection occasion j and in state s at detection occasion $j + 1$ and 0 otherwise. Note that $w_{i,j,r,\dagger}$ is 1 if individual i dies between j and $j + 1$, $w_{i,j,r,\cdot} = \sum_{s \in R_{j+1}} w_{i,j,r,s}$ is 1 if the individual survives, and the dot represents any state but the death state.

We modeled reach-specific travel times using a lognormal distribution because travel times of migrating juvenile salmon are typically right-skewed, and the lognormal distribution often fits travel time data well (Muthukumarana et al. 2008). Missing travel times (i.e., $t_{i,r,j} = NA$) are imputed from a lognormal distribution subject to the constraint

$$(8) \quad T_{i,j+K} = T_{i,j} + \sum_{k=0}^{K-1} t_{i,r,j+k}^{\text{mis}}$$

where $T_{i,j}$ and $T_{i,j+K}$ are observed cumulative travel times, $t_{i,r,j}^{\text{mis}}$ are missing reach-specific travel times between occasions j and $j + K$, and K is the number of missing reach-specific travel times between $T_{i,j}$ and $T_{i,j+K}$ ($K = 2, \dots, J - 1$). Since the sum of missing travel times are constrained to be equal to $T_{i,j+K} - T_{i,j}$, this constraint on imputed travel times imposes a form of left-censoring, thereby providing additional information to the parameter estimation.

Given observed and imputed travel times, the complete data likelihood for the travel time data are

$$(9) \quad L[\mu, \sigma | t^{\text{obs}}, t^{\text{mis}}] \propto \prod_{i=1}^N \prod_{j=F_i}^{J-1} \prod_{r \in R_j} \frac{1}{\sigma_{i,r,j}^2 t_{i,r,j}} \exp \left\{ -\frac{[\ln(t_{i,r,j}) - \mu_{i,r,j}]^2}{2\sigma_{i,r,j}^2} \right\}$$

where $t_{i,r,j}$ is the observed (t^{obs}) or imputed (t^{mis}) travel time for individual i in state r at detection occasion j , and $\sigma_{i,r,j}^2$ is the variance of the lognormal travel time distribution for individual i in state r at occasion j . We estimated $\sigma_{i,r,j}^2$ as a constant over all individuals for each reach.

Other parameter constraints

In addition to constraining parameters as a function of covariates, a number of other constraints were imposed owing to telemetry station outages, multiple release locations, and parameter identifiability issues.

For reach 0, individuals were either released at Sacramento (rkm 172), at rkm 191, or well upstream of these locations (>rkm 191; Table 1). For fish released well upstream of Sacramento, we included in the analysis only those that were detected by telemetry stations in the vicinity of Sacramento or at a telemetry station located near the Feather River at rkm 204 (see “number analyzed” in Table 1). To account for the effect of detection or release upstream of Sacramento on travel times through reach 0, we included coefficients that estimated the difference in intercepts for fish detected at rkm 204 or released at rkm 191 relative to those detected or released at Sacramento (rkm 172).

We treated the first reach after release as an “acclimation” reach to allow fish to recover from handling and release procedures before drawing inferences about travel time and survival (reach 0 for releases at Sacramento and reach 5 for releases in Georgiana Slough). Therefore, fish released directly into Georgiana Slough (rkm 115; Table 1) were modeled with unique coefficient values in reach 5 relative to fish that entered reach 5 volitionally from upstream locations. Coefficients based only on fish that entered reach 5 volitionally were then used for inference about travel time and survival in reach 5.

Telemetry station A_3 was not deployed until January 2007, affecting release 1, and was not deployed between December 2007 and March 2008, affecting releases 4–7. To incorporate the effect of these receiver outages, detection probability was set to 0 for fish that were imputed to arrive at site A_3 during these time periods. In preliminary analysis, we found coefficients associated with survival in reach 2 were weakly identifiable (i.e., large credible intervals), and we identified undue influence of the prior distribution on U , the upper limit of the logistic function for routing into Sutter and Steamboat Slough (Ψ_{AB3}). Both issues were likely driven by the extended receiver outages at telemetry station A_3 . Therefore, we set all survival coefficients for reach 2 equal to those for reach 1 and estimated common slopes, intercepts, and random-effects parameters. This constraint was supported by previous analyses showing similar survival between reaches 1 and 2 (Perry 2010; Perry et al. 2010).

For routing into Sutter and Steamboat Slough, we included auxiliary data from an independent telemetry study to bolster parameter estimates associated with Ψ_{AB3} (California Department of Water Resources 2016; Romine et al. 2017). Of 4528 acoustically tagged juvenile late-fall Chinook salmon released at Sacramento between 1 March and 15 April 2014, 3548 fish were detected at the junction of the Sacramento River and Sutter and Steamboat Slough. We modeled this binary data (1 = Sutter and Steamboat Slough, 0 = Sacramento River) using a Bernoulli likelihood with probability Ψ_{AB3} and jointly estimated the parameters of eq. 4 for Ψ_{AB3} over both data sets.

Last, unique detection probabilities could not be estimated at the entrance to the Delta Cross Channel (telemetry station C_4) and Georgiana Slough (telemetry station D_4) owing to a single downstream detection site common to both reaches (telemetry station D_5). Therefore, a common set of coefficients for detection probability were estimated for sites D_4 and C_4 .

Prior distributions, parameter estimation, and goodness of fit

Prior distributions for parameters associated with routing, survival, and detection were based on the default priors for logistic regression recommended by Gelman et al. (2013). First, all continuous covariates were scaled to have mean 0 and standard deviation 0.5 (for discharge, Q , mean = 610.1 m³·s⁻¹, SD = 407.1 m³·s⁻¹; for fork length, l , mean = 155.1 mm, SD = 10.8 mm). Next, slope parameters associated with routing, survival, and detection were drawn from a Student’s t distribution with a mean of 0, standard deviation of 2.5, and 7 degrees of freedom. Intercepts associated with routing, survival, and detection were drawn from a Cauchy(0, 10) distribution. We used a Normal(0, 1) distribution truncated at zero as the prior distribution for ξ_s and ξ_ψ (Gelman et al. 2013). Last, a Uniform(0, 1) prior was used for L and U . For travel time parameters, slopes and intercepts for μ were drawn from a Normal(0, 10) prior distribution, and ξ_μ and σ were drawn from a Uniform(0, 10) prior.

We coded the model in the MCMC software package JAGS (<http://mcmc-jags.sourceforge.net/>) as called from R (Denwood 2016), which allowed us to simultaneously estimate all model parameters and impute missing data (see Supplement B¹). JAGS uses Gibbs sampling and Metropolis–Hastings methods to sequentially update each parameter value, conditional on the current value for all other parameters. We ran three MCMC chains in JAGS each for 50 000 iterations that consisted of a 1000 iteration adaptation phase and an additional 30 000 iteration burn-in phase. The final 20 000 iterations were thinned at a rate of 1 in 20 resulting in 1000 iterations from each chain that were used to form the joint posterior distribution of the parameters. With these MCMC settings, the model took 5 days to run (10 000 iterations per day) on a desktop computer with a 3.5 GHz processor and 64 GB of RAM.

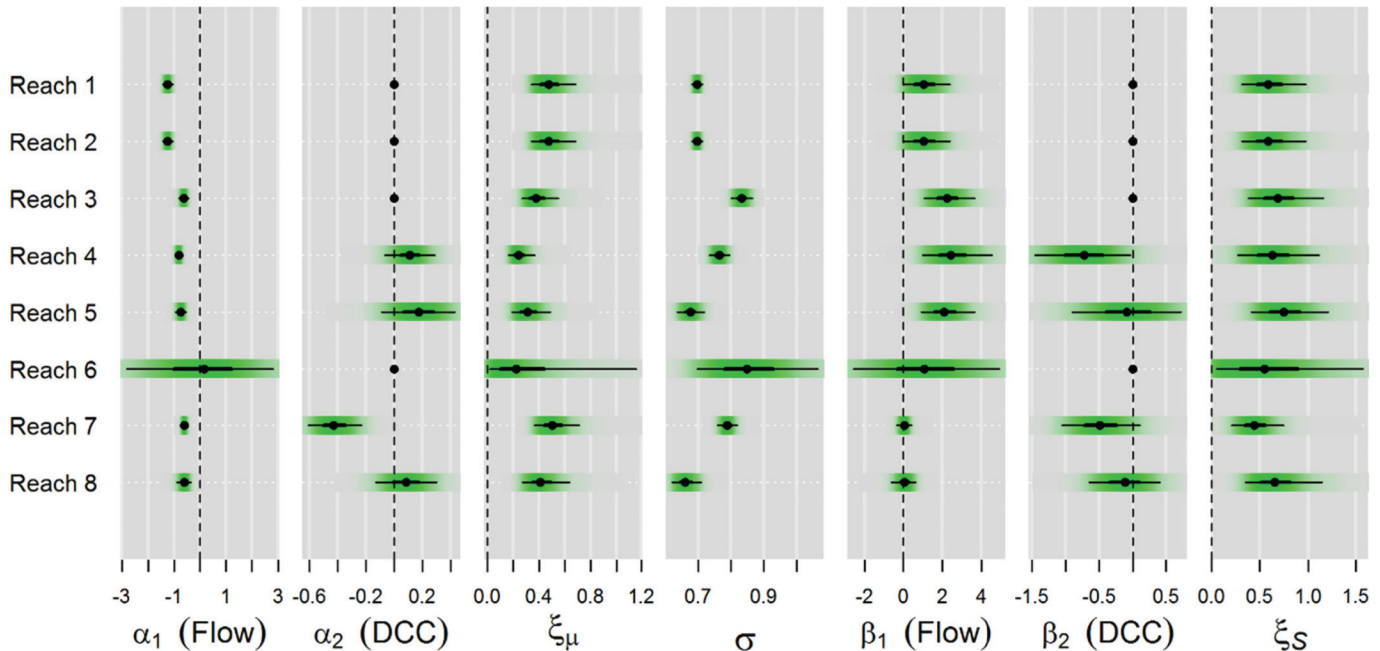
We inspected trace plots of each MCMC chain and used the \hat{R} statistic to assess convergence of the posterior for each parameter, where $\hat{R} < 1.1$ indicates convergence (Gelman et al. 2013). We then performed posterior predictive checks to assess goodness of fit by simulating replicated data from the joint posterior distribution. We used the joint log-likelihood of the capture histories (eq. 7) and travel times (eq. 9) as a goodness of fit statistic, which was calculated for both observed and replicated data for each draw in the joint posterior distribution. We calculated the probability that the observed data could have been generated by the model by calculating the proportion of times that the likelihood of the observed data was greater than that for replicated data. Often referred to as a Bayesian p value, a probability >0.95 or <0.05 is typically taken as evidence of lack of fit (Gelman et al. 2013).

Results

The \hat{R} statistics indicated that the Markov chains converged to a stable stationary distribution. Of the 155 estimated parameters, \hat{R}

Can. J. Fish. Aquat. Sci. Downloaded from www.nrcresearchpress.com by CA DEPARTMENT OF FISH AND WILDLIFE on 08/02/19 For personal use only.

Fig. 4. Summary of posterior distributions of parameters estimating the effects of river flow and Delta Cross Channel (DCC) gate position on travel time and survival. Points show the median of the posterior distribution, heavy lines show the 25th to 75th percentiles, and thin lines show the 5th to 95th percentiles. Green bars are density strips, with darker regions illustrating higher posterior density. Parameter definitions are as follows: α_1 = slope for effect of discharge on mean of log-travel time, α_2 = slope for effect of an open DCC gate on mean of log-travel time, ξ_μ = standard deviation of release group random effect on μ , σ = variance parameter of the lognormal travel time distribution, β_1 = slope for effect of discharge on survival, β_2 = slope for effect of an open DCC gate on survival, ξ_s = standard deviation of release group random effect on survival. [Colour online.]



was less than 1.1 for all but one parameter ($\theta_{0,D4,4}$, the intercept for P at telemetry station D_4 in year 4), and its \hat{R} was 1.115, just slightly higher than the standard cutoff value. In addition, we found no evidence of lack of fit; 54.4% of log-likelihood values for the observed data were greater than those for replicated data, indicating that the observed data were just as likely to have been generated by the model compared with replicated data that was known to have been generated by the model.

Daily inflow to the Delta varied widely over the study period, ranging from 193 to 2180 $\text{m}^3 \cdot \text{s}^{-1}$ (Fig. 3), which encompassed the 1st to 95th percentiles of daily discharge in the 69-year flow record for the December through March migration period. Inflows influenced detection probabilities, travel time, survival, and routing. We found that discharge had a negative effect on detection probabilities at most telemetry stations, but the magnitude of the effect declined from the upper to lower Delta as tidal influence increased (Fig. S3¹). In general, detection probabilities were greater than 0.8 at most telemetry stations when flows were below 1000 $\text{m}^3 \cdot \text{s}^{-1}$, but decreased at higher flows with the rate of decrease varying among years and telemetry stations (Fig. S4¹).

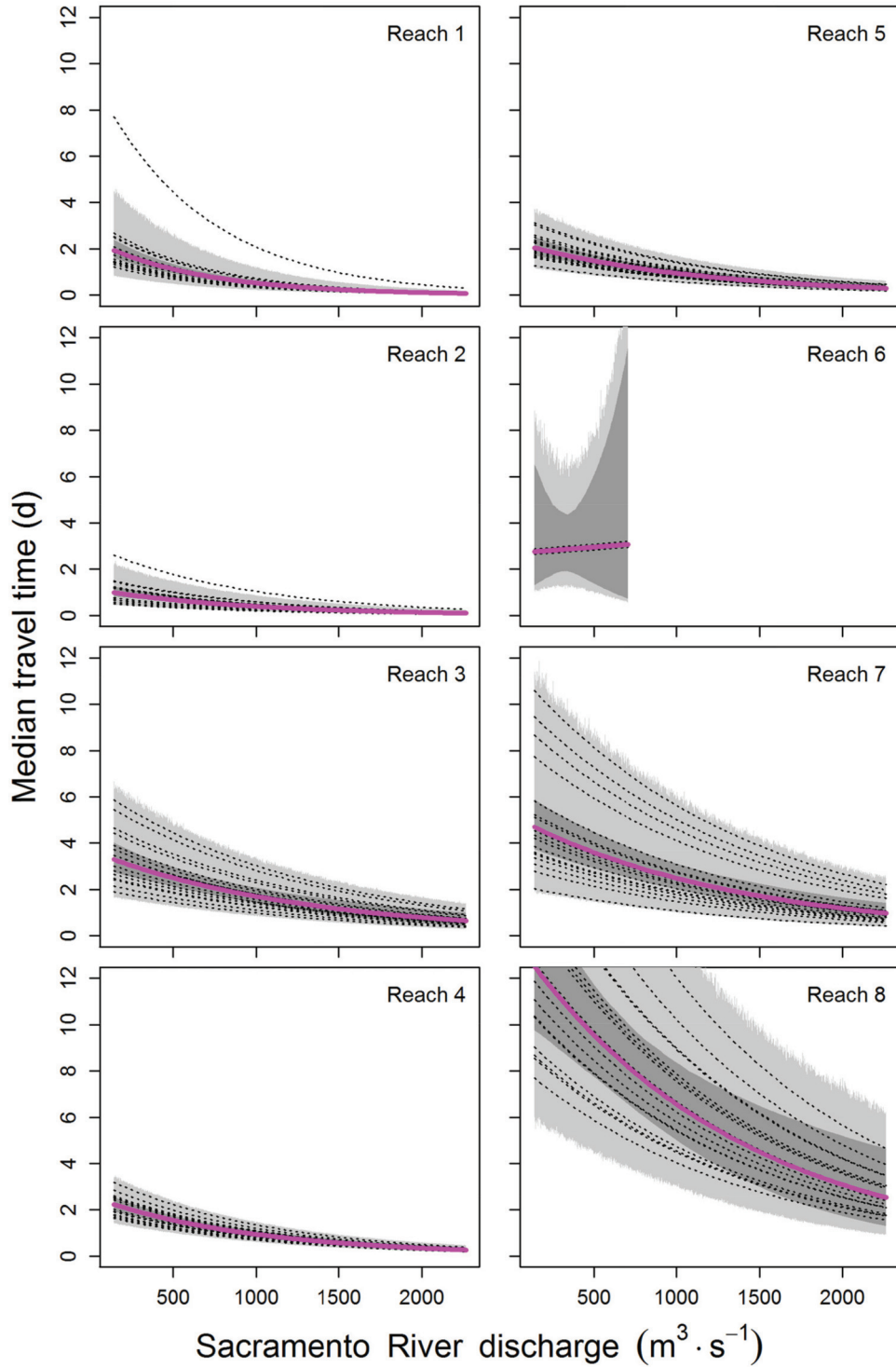
Most survival and travel time parameters associated with reach 6 (the Delta Cross Channel) exhibited wide credible intervals because only six release groups were released prior to mid-December when the Delta Cross Channel undergoes mandatory closures for fish protection (Fig. 4). Consequently, there was relatively little data from which to estimate the effects of river discharge on travel time and survival for reach 6.

For all other reaches, we found that median travel time was influenced by river flow. Posterior distributions for the effect of flow on travel time (α_1) were negative and credible intervals excluded zero, indicating that increases in river flow reduced median travel times (Figs. 4 and 5). Credible intervals for the effect of the Delta Cross Channel on median travel time (α_2) overlapped 0, with the exception of reach 7, indicating little evidence for an

effect of an open gate on travel time (Fig. 4). Credible intervals for the standard deviation of the release-group random effects (ξ_μ) were well above 0, providing evidence that median travel times varied among release groups after accounting for other effects in the model. At low inflows, median travel times for tidal reaches (reaches 7 and 8) were considerably longer than other reaches (Fig. 5). Furthermore, at low flows, median travel times for reach 8 were about 2.5 times that of reach 7.

In contrast with travel time, survival was strongly related to river flow in just three of eight reaches. In the upper two reaches, which exhibit the least tidal influence, the effect of flow (β_1) was positive (Fig. 4), but the relative change in survival was small because survival was >0.90 over the range of observed discharge (Fig. 6). However, we estimated strong positive effects of river flow in reaches 3–5 (Fig. 4); these reaches transition from bidirectional to unidirectional flow as river discharge increases (Fig. 3, middle panel). Although discharge affected travel time in the tidal reaches (reaches 7 and 8), the posterior distributions of β_1 were centered on 0 for these reaches and credible intervals were narrow, providing strong evidence of little relationship between survival and discharge. We also found evidence that operation of the Delta Cross Channel, which removes water from the Sacramento River downstream of the Delta Cross Channel (reaches 4 and 7). For these reaches, posterior medians of β_2 were negative, and 75%–90% of the posterior distribution was less than 0 (Fig. 4). Similar to findings with travel time, the posterior distributions for standard deviations of random effects associated with survival were positive, indicating additional release-to-release variation in survival over and above the effects of covariates included in the model. Last, we also found a positive effect of fork length on survival (β_3 , median = 0.152, 90% credible interval = 0.062–0.243; Fig. S5¹).

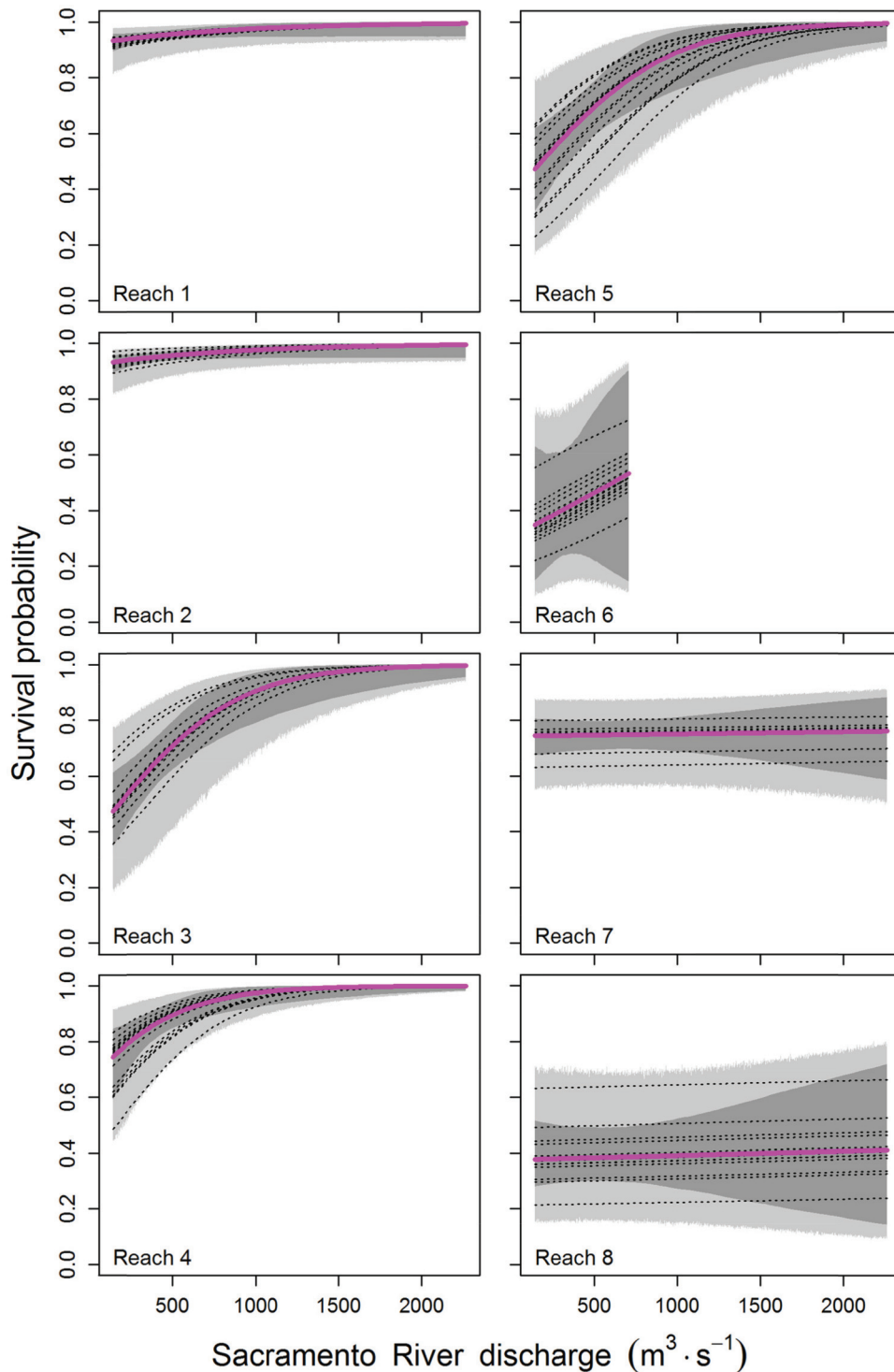
Fig. 5. Reach-specific relationships between median travel time and inflow to the Delta as measured at the Sacramento River at Freeport (shown for closed Delta Cross Channel gates). The heavy magenta line shows the mean relationship, and the dotted lines show the random effects estimates for each release group based on medians of the joint posterior distribution. The dark gray region shows 95% credible intervals about the mean relationship. The light gray region shows the 95% confidence interval among release groups. [Colour online.]



Reach-specific flow–survival relationships revealed that survival increased sharply with river flow in transitional reaches but not riverine or tidal reaches (Fig. 6). Survival in riverine reaches (reaches 1 and 2) were high regardless of discharge, approaching 1 as flow increased. In transitional reaches, median survival at the lowest flows was about 0.75 for reach 4 (Sacramento River) and 0.5 for reach 3 (Sutter and Steamboat Slough) and reach 5 (Georgiana

Slough). In these reaches, survival increased sharply with river flow, approaching 1 as river flow exceeded 1000 $\text{m}^3 \cdot \text{s}^{-1}$, which coincides with the transition from bidirectional to unidirectional flow (Fig. 3, middle panel). In tidal reaches, survival was not related to discharge, but median survival in reach 7 (Sacramento River) was about twice that observed in reach 8 (interior Delta).

Fig. 6. Reach-specific relationships between survival and inflow to the Delta as measured at the Sacramento River at Freeport (shown for closed Delta Cross Channel gates and plotted at the mean fork length). The heavy magenta line shows the mean relationship, and dotted lines show the random effects estimates for each release group based on medians of the joint posterior distribution. The dark gray region shows 95% credible intervals about the mean relationship. The light gray region shows the 95% confidence interval among release groups. [Colour online.]



We found that routing probabilities (Fig. 7) followed a relationship similar to that between total discharge (Q) and the fraction of discharge entering each route (Fig. S2¹), indicating that the distribution of mean daily flow among channels is a key driver of migration routing (see also Cavallo et al. 2015). As discharge increases, the probability of entering Sutter and Steamboat Slough

increased by 12 percentage points from about 0.23 to an estimated upper limit (U) of 0.35 (Table 2; Fig. 7). In contrast, as flow increases, the probability of entering Georgiana Slough (when the Delta Cross Channel gate is closed) decreased by 16 percentage points from 0.43 to an estimated lower limit (L) of 0.27 (Table 2; Fig. 7). For these routes, routing probabilities approach upper and lower lim-

Fig. 7. Relationships between routing probability and inflow to the Delta as measured at the Sacramento River at Freeport (A_2 in Fig. 1). The lower right panel shows the effect of Delta Cross Channel (DCC) gate position on routing probabilities at the junction of the Sacramento River, DCC, and Georgiana Slough (A_4 , C_4 , and D_4 in Fig. 1), plotted at the posterior median of the parameters. Other panels show mean routing relationships (heavy magenta line), random effects estimates for each release group (dotted lines), 95% credible interval about the mean relationship (dark gray region), and 95% confidence interval among release groups (light gray region). [Colour online.]

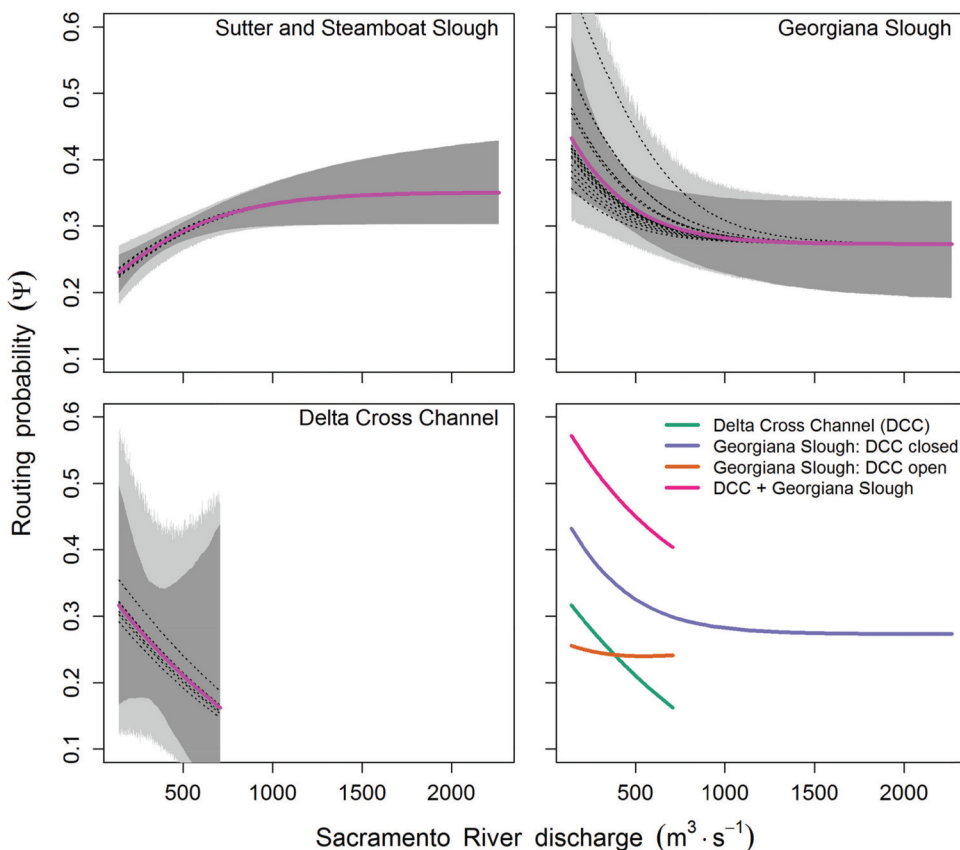


Table 2. Posterior medians (90% credible intervals) for routing probabilities expressed as a function of time-varying individual covariates.

Parameter	Sutter and Steamboat Slough (Ψ_{AB3})	Delta Cross Channel (Ψ_{AC4})	Georgiana Slough (Ψ_{AD4C})
U	0.35 (0.31–0.43)	1	1
L	0	0	0.27 (0.20–0.32)
γ_0	1.89 (0.91–3.30)	-1.49 (-2.40– -0.67)	-2.95 (-4.57– -1.83)
γ_1	2.17 (1.10–4.15)	-1.25 (-3.47–0.90)	-6.53 (-5.46– -1.24)
γ_2	0	0	-0.55 (-2.76–0.33)
ξ_Ψ	0.19 (0.04–0.50)	0.31 (0.06–0.87)	0.89 (0.46–1.58)

Note: U = upper limit of logistic function, L = lower limit of logistic function, γ_0 = intercept, γ_1 = slope for effect of discharge on routing, γ_2 = slope for effect of open Delta Cross Channel gates on routing, ξ_Ψ = standard deviation of the release group random effect. Parameter values without associated credible intervals were set to the given value.

its at an inflow of about $1000 \text{ m}^3\cdot\text{s}^{-1}$ (Fig. 7), the point at which transitional reaches switch from bidirectional to unidirectional flows (Fig. 3, middle panel). We found little variation in routing probability among release groups for Sutter and Steamboat Slough and the Delta Cross Channel, but considerable variation for Georgiana Slough, particularly at low discharge (Fig. 7).

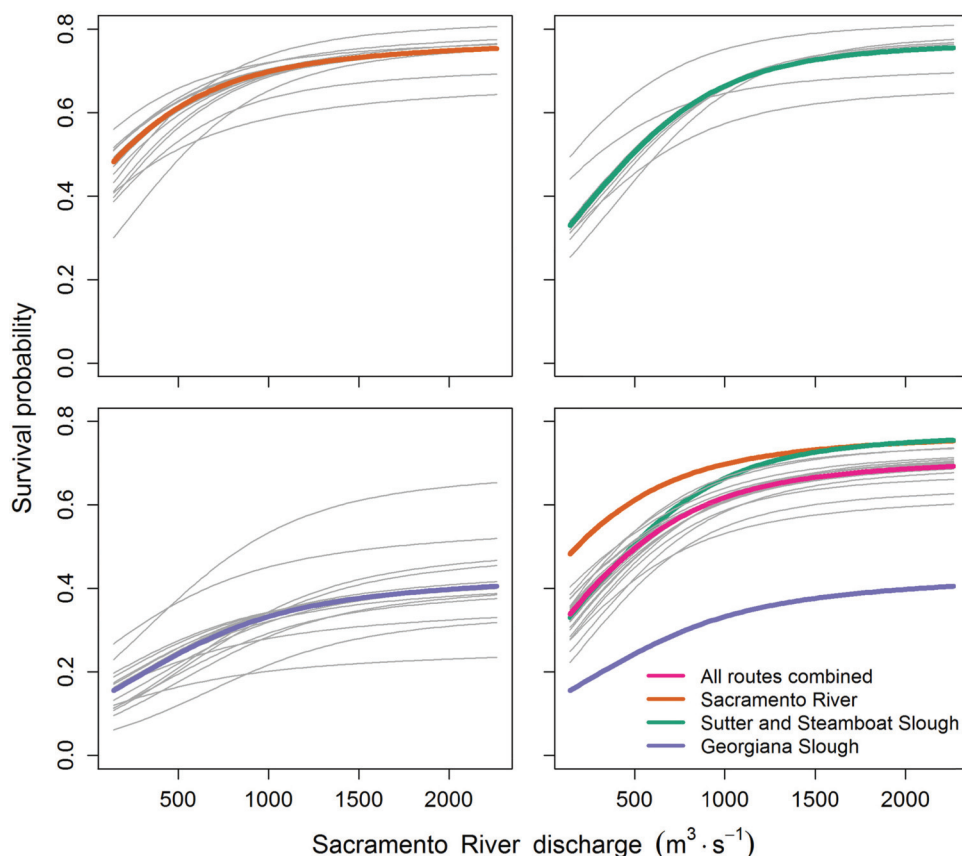
We found that operation of the Delta Cross Channel increased the proportion of fish migrating through interior Delta (reach 8) where survival is low. Routing into the Delta Cross Channel decreased as flow increased, although credible intervals were wide (Table 2; Fig. 7). We found evidence that an open Delta Cross gate reduced the probability of entering Georgiana Slough (Table 2;

Fig. 7, lower right panel). However, the combined probability of entering Georgiana Slough and Delta Cross Channel, both of which lead fish to the interior Delta (reach 8), was 15 percentage points higher than the probability of entering Georgiana Slough alone when the gates are closed (Fig. 7, lower right panel).

The reach-specific survival relationships with flow dictate the composite survival of juvenile salmon migrating through the Delta via alternative migration routes. At low flows, fish migrating through the Sacramento River exhibit the highest through-Delta survival, followed by Sutter and Steamboat Slough, but as river discharge increases, survival for Sutter and Steamboat Slough approaches that of the Sacramento River, leveling off at a survival of about 0.75 (Fig. 8). Survival of fish migrating through Georgiana Slough also increases with inflow but approaches a maximum of about 0.4. Since survival in all reaches except 7 and 8 approaches 1 as discharge increases, survival in the tidal reaches imposes an upper limit on the overall through-Delta flow–survival relationship for each route.

Since routing probabilities determine the fraction of the population experiencing a given route-specific survival, both factors contribute to the shape of the relationship between overall survival and discharge. Mean overall survival increases with discharge from about 0.32 to 0.70 and falls in between the route-specific survival relationships (Fig. 8, lower right panel). However, at low flows, overall survival is pulled more towards the low survival of Georgiana Slough (Fig. 8, lower right panel) because the proportion of fish entering Georgiana Slough is highest at low flows (Fig. 7). By contrast, as the proportion of fish entering Georgiana Slough decreases with increasing flow, overall survival not

Fig. 8. Route-specific survival through the Sacramento–San Joaquin River Delta between Freeport (A_2 in Fig. 1) and Chipps Island (A_6 in Fig. 1). Route-specific survival based on posterior median parameter values was calculated as the product of reach-specific survival for reaches that trace each unique migration route through the Delta (shown for closed Delta Cross Channel gates). The first three panels show the mean relationship for each route, with thin gray lines showing the random effects estimates for each release group. The bottom right panel shows overall survival through Delta for all routes (with random effects estimates as thin gray lines) along with route-specific survival relationships. Overall survival was calculated as the average of route-specific survival weighted by routing probabilities (see eq. 1). [Colour online.]



only increases owing to the flow–survival relationships, but is weighted more towards the higher-survival migration routes owing to the flow-routing relationships.

Route-specific travel time distributions also vary considerably with river flow, and fish traveling through the interior Delta (reach 8) via Georgiana Slough or the Delta Cross Channel exhibit longer travel times than those that migrate through the north Delta via the Sacramento River and Sutter and Steamboat Slough (Fig. 9). For example, at inflows of $235 \text{ m}^3 \cdot \text{s}^{-1}$, the median travel time for Georgiana Slough is 18.0 days, with some travel times as long as 40 days. By comparison, for north Delta routes, median travel times are 12.2–12.6 days, with the tail of the distribution extending to 30 days. In contrast, at inflows of $1357 \text{ m}^3 \cdot \text{s}^{-1}$, expected median travel times are 2.7–3.1 days for north Delta routes compared with 6.4 days for Georgiana Slough, with a 10-day difference between the tails of the distributions.

Discussion

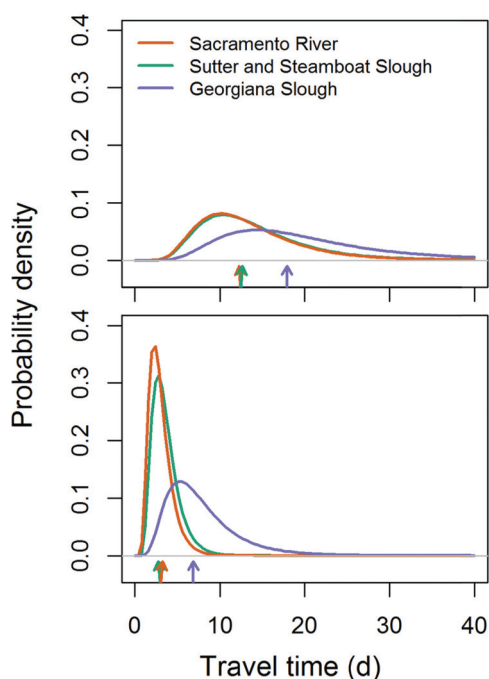
Understanding spatiotemporal variation in survival of migrating populations is critical for identifying underlying mechanisms driving survival, particularly in a highly dynamic and spatially complex environment such as the Sacramento–San Joaquin River Delta. Although variation in survival of juvenile salmon migrating through the Delta has long been linked to freshwater inflows (Kjelson and Brandes 1989; Newman and Rice 2002; Newman 2003), we lacked understanding of how spatial variation in survival gave rise to this overall relationship. Our analysis has revealed that the overall flow–survival relationship is driven by

three key reaches that transition from unidirectional flow at high inflows to tidally driven bidirectional flow at low inflows. In contrast, riverine reaches exhibited high survival at all levels of inflow, and tidal reaches had lower but constant survival with respect to inflow. Thus, the flow–survival relationship captures the gradient that occurs as transitional reaches shift from tidal to riverine environments as inflow increases.

In addition to being the hub of California's water delivery system, the Delta forms a critical nexus between freshwater and ocean environments. Juvenile salmon emigrating from natal tributaries first experience a tidal environment during their migration through the Delta. Juvenile salmon are particularly vulnerable during this transition because they must modify their migration tactics to progress seaward while undergoing physiological changes in preparation for seawater entry. Although some researchers have found high survival rates in estuaries (Clark et al. 2016), others have found that migration through estuaries is associated with high mortality rates relative to riverine or early marine phases (Thorstad et al. 2012 and references therein). For example, in a study of juvenile Atlantic salmon (*Salmo salar*) in riverine, estuarine, and early ocean environments, Halfyard et al. (2013) found that survival was most impacted in estuarine habitats near the head of tide. Our study is consistent with these findings and highlights how river inflows can interact with tides to influence survival by shifting the location at which the hydrodynamics switch from unidirectional to bidirectional flow.

Many studies (ours included) have correlated travel time and survival to river flow because these relationships provide a direct

Fig. 9. Route-specific travel time distributions between Freeport (A_2 in Fig. 1) and Chipps Island (A_6 in Fig. 1) at the 5th (top panel) and 95th (bottom panel) percentiles of discharge based on the historical flow record (235 and 1357 $\text{m}^3\cdot\text{s}^{-1}$, respectively). Arrows show the median travel times for each route. Travel time distributions were based on posterior medians of parameters for reach-specific travel time distributions assuming closed Delta Cross Channel gates. [Colour online.]



linkage between a key management variable and the subsequent response of migrating juvenile salmon populations (Connor et al. 2003; Smith et al. 2003; Courter et al. 2016). However, it is important to recognize that river flow affects travel time and survival through both direct and indirect mechanisms. River flow directly influences migration rates of juvenile salmon by dictating water velocity, which is a function of channel geometry (Zabel and Anderson 1997; Zabel 2002; Tiffan et al. 2009). In turn, migration rates dictate arrival timing at ocean entry, which can influence early ocean survival (Satterthwaite et al. 2014). In contrast, river flow affects survival indirectly through a number of possible mechanisms. River flow can affect the proportion of fish using alternative routes at hydroelectric projects (Coutant and Whitney 2000) and in channel network systems such as the Delta (Cavallo et al. 2015; Perry et al. 2015). If survival differs among routes, which is often the case, then river discharge affects population survival by influencing the proportion of fish using high- or low-survival routes (Perry et al. 2013, 2016). In addition, river flow is often correlated with other environmental variables that influence survival such as turbidity and water temperature (Baker et al. 1995; Connor et al. 2003; Smith et al. 2003), which in turn may influence predation rates (Vogel and Beauchamp 1999; Ferrari et al. 2013).

Reducing travel time and exposure to predators is a key mechanism by which river flow has been hypothesized to affect survival of migrating juvenile salmonids, but establishing this linkage has proven elusive. Although travel time has been consistently linked with discharge via water velocity, some studies in the Snake and Columbia rivers found no significant relationship between travel time and survival but a significant relation between migration distance and survival (Bickford and Skalski 2000; Smith et al. 2002). To explain these counterintuitive findings,

Anderson et al. (2005) developed a predator–prey model that expressed survival as a function of both travel time and travel distance. Their analysis revealed that the dependence of survival on travel time is dictated by the nature of predator–prey interactions. When prey migrate in a directed fashion through a field of stationary predators, survival is independent of travel time and depends only on travel distance. In contrast, survival depends on travel time when random movement dominates directed migration or when predators adopt prey searching tactics. These findings illustrate how the relationship between flow and survival is context-dependent, arising from a combination of mechanisms that may directly affect survival (e.g., temperature) or indirectly affect survival by modifying predator encounter rates (temperature, turbidity, predator and prey behavior). Although our analysis here focused on estimating the association between discharge and survival, our modeling framework allows exploration of alternative model structures for linking flow to survival via travel time. For example, the XT model can be incorporated into our analytical framework and compared against the current model structure to assess the strength of evidence for the dependence of survival on travel time.

Predation by a host of non-native piscivorous fishes is thought to be the primary proximate cause of juvenile salmon mortality in the Delta (Cavallo et al. 2013; Grossman 2016; Sabal et al. 2016). Variation in survival among reaches observed in our study is consistent with expectations based on predator–prey models. Juvenile salmon migrate downstream through riverine reaches in a directed fashion, and survival was high regardless of inflows and variation in travel time. We observed a similar pattern at high flows when transitional reaches exhibit unidirectional flows similar to riverine reaches. As inflow declines and tidal influence moves upstream into transitional reaches, not only does travel time increase but travel distance increases because juvenile salmon may be advected upstream on flood tides (Moser et al. 1991). Simultaneously increasing both travel time and cumulative travel distance will act to increase predator encounter rates. Thus, the flow–survival relationship that we observed in transitional reaches likely arises from the transition from directed downstream movement at high flows to less directed, bidirectional movement during low flows. In tidal reaches, our a priori expectation was that neither travel time nor survival would be related to inflow because the magnitude of tidal flows (on the order of $\pm 3500 \text{ m}^3\cdot\text{s}^{-1}$) swamps the signal of net inflow (Fig. 3, bottom panel). Although we observed no relation between survival and inflow in tidal reaches, we were surprised to find a strong effect of inflow on travel time, suggesting that survival may be decoupled from travel time in tidal reaches.

We included only inflow, Delta Cross Channel gate position, and fork length as covariates on reach-specific survival, but numerous other factors drive variation in survival. By casting our mark–recapture model in a hierarchical Bayesian framework and including a random effect on release group, we were able to quantify the magnitude of this variation but not its source. Seasonal and annual variation in reach-specific predator densities, environmental drivers (e.g., water temperature, turbidity), and spring-neap tidal cycles will act to modulate how travel time and survival respond to changes in inflow, thereby propagating variation among cohorts of juvenile salmon that experience a common set of flow conditions. Specifically, variation in survival among release groups was highest in tidal reaches and in transition reaches during low inflows, further suggesting that tidal cycles play an important role in driving variation in survival. For example, at a given inflow, cohorts migrating through the Delta during neap tides will experience lower-magnitude flood tides and first encounter bidirectional flows further downstream relative to cohorts migrating during spring tides. The high release-to-release variation in our study provides opportunity for future work to

quantify how factors other than inflow influence survival in the Delta.

Our Bayesian mark–recapture model makes two important advances in the development of statistical mark–recapture models used to estimate survival of migrating juvenile salmonids. First, modeling individual covariates that vary through time is challenging owing to missing covariate values for undetected individuals. Consequently, most approaches have ignored within- and among-individual variation by averaging covariates over individuals within release groups (Connor et al. 2003; Smith et al. 2003) or averaging covariates over space and time for each individual (Stich et al. 2015). In contrast, our model allows for individual covariates that vary through space and time by incorporating an auxiliary model for travel times to impute missing travel time, reach entry times, and covariates at the time of reach entry. Given the considerable capital expense associated with conducting telemetry studies, our framework allows the maximum amount of information to be extracted from telemetry data sets that typically have small sample sizes. Second, our joint travel time and mark–recapture model explicitly considers both migration and demographic processes under a single analytical framework. Thus, our modeling framework opens the door to a number of useful extensions such as modeling survival directly as a function of an individual's travel time (Muthukumarana et al. 2008) or by using an event-time framework (e.g., Sparling et al. 2006; Zabel et al. 2014) where survival can be modeled as a function of temporal variation in covariates during an individual's residence time within a reach.

Our analysis provides insight into how water management decisions that influence inflow and water routing are likely to affect travel time, routing, and survival of migrating juvenile salmonids. First, survival decreases sharply and routing into the interior Delta (where survival is low) increases sharply as Delta inflows decline below approximately $1000 \text{ m}^3 \cdot \text{s}^{-1}$, the point at which transitional reaches shift from bidirectional to unidirectional flow (Figs. 7 and 8). In contrast, at inflows greater than $1000 \text{ m}^3 \cdot \text{s}^{-1}$, survival is maximized and changes relatively little with flow while routing into the interior Delta via Georgiana Slough is minimized and insensitive to inflow. These findings indicate that water management actions that reduce inflows to the Delta will have relatively little effect on survival at high flows, but potentially considerable negative effects at low flows. Furthermore, operation of the Delta Cross Channel not only increases the fraction of the population that enters the interior Delta where survival is low (Fig. 7), but is associated with lower survival for the Sacramento River (Fig. 4). These compounding effects of opening the Delta Cross Channel act to further reduce overall survival relative to inflows alone (Fig. S6¹). Our findings illustrate how trade-offs between juvenile salmon survival and water management for human use vary with the amount of flow entering the Delta. Thus, our modeling framework can be used as a management tool to explore the consequences of such trade-offs and to quantitatively assess the effect of alternative management scenarios on travel time, routing, and survival.

Water flow has been dubbed the “master” variable in the Delta because of its economic importance and its pervasive effect on all components of this complex and dynamic aquatic ecosystem (Mount et al. 2012; Lund et al. 2015). Indeed, our work is beginning to shed light on the multiple ways in which river flows differentially affect survival in different reaches of the Delta and interact with water and fish routing to affect overall survival. In turn, these insights will aid managers in devising strategies to balance consumptive water use with management actions that aim to recover threatened and endangered salmon populations in the Sacramento River.

Acknowledgements

Funding for this study was provided by the Delta Stewardship Council, Grant 2045 (RWP and PLB, principal investigators). We are grateful to the many field biologists who helped to collect the data upon which our analysis was based. Special thanks are extended to the staff of the Coleman National Fish Hatchery for logistical support and for providing the juvenile salmon used in our analysis. Amy Hansen, Ken Tiffan, and Josh Korman provided many insightful comments that improved the manuscript. Any use of trade, firm, or product names is for descriptive purposes only and does not imply endorsement by the US Government.

References

- Anderson, J.J., Garraie, E., and Zabel, R.W. 2005. Mean free-path length theory of predator–prey interactions: application to juvenile salmon migration. *Ecol. Modell.* **186**(2): 196–211. doi:10.1016/j.ecolmodel.2005.01.014.
- Baker, P.F., Ligon, F.K., and Speed, T.P. 1995. Estimating the influence of temperature on the survival of Chinook salmon smolts (*Oncorhynchus tshawytscha*) migrating through the Sacramento–San Joaquin River Delta of California. *Can. J. Fish. Aquat. Sci.* **52**(4): 855–863. doi:10.1139/f95-085.
- Bickford, S.A., and Skalski, J.R. 2000. Reanalysis and interpretation of 25 years of Snake–Columbia River juvenile salmonid survival studies. *N. Am. J. Fish. Manage.* **20**(1): 53–68. doi:10.1577/1548-8675(2000)020<0053:RAIOYO>2.0.CO;2.
- Bonner, S.J., and Schwarz, C.J. 2004. Continuous time-dependent individual covariates and the Cormack–Jolly–Seber model. *Anim. Biodivers. Conserv.* **27**(1): 49–155.
- Brandes, P.L., and McLain, J.S. 2001. Juvenile Chinook salmon abundance, distribution, and survival in the Sacramento–San Joaquin Estuary. In *Contributions to the Biology of the Central Valley Salmonids*, Fish Bulletin 179, Vol. 2. Edited by R.L. Brown. California Department of Fish and Game, Sacramento, Calif. pp. 39–138.
- California Department of Water Resources. 2016. 2014 Georgiana Slough Floating Fish Guidance Structure Performance Evaluation Project Report [online]. Bay-Delta Office, Sacramento, California. Available from <http://baydeltaoffice.water.ca.gov/sdb/GS/docs/Final%20Report%20October%202016%20Edition%20103116-signed.pdf> [accessed 22 November 2017].
- Catchpole, E.A., Morgan, B.J., and Tavecchia, G. 2008. A new method for analysing discrete life history data with missing covariate values. *J. R. Stat. Soc. B.* **70**(2): 445–460. doi:10.1111/j.1467-9868.2007.00644.x.
- Cavallo, B., Merz, J., and Setka, J. 2013. Effects of predator and flow manipulation on Chinook salmon (*Oncorhynchus tshawytscha*) survival in an imperiled estuary. *Environ. Biol. Fishes.* **96**(2–3): 393–403. doi:10.1007/s10641-012-9993-5.
- Cavallo, B., Gaskill, P., Melgo, J., and Zeug, S.C. 2015. Predicting juvenile Chinook Salmon routing in riverine and tidal channels of a freshwater estuary. *Environ. Biol. Fishes.* **98**(6): 1571–1582. doi:10.1007/s10641-015-0383-7.
- Clark, T.D., Furey, N.B., Rechisky, E.L., Gale, M.K., Jeffries, K.M., Porter, A.D., Casselman, M.T., Lotto, A.G., Patterson, D.A., Cooke, S.J., Farrell, A.P., Welch, D.W., and Hinch, S.G. 2016. Tracking wild sockeye salmon smolts to the ocean reveals distinct regions of nocturnal movement and high mortality. *Ecol. Appl.* **26**(4): 959–978. doi:10.1890/15-0632. PMID:27509741.
- Connor, W.P., Burge, H.L., Yearsley, J.R., and Bjornn, T.C. 2003. Influence of flow and temperature on survival of wild subyearling fall Chinook salmon in the Snake River. *N. Am. J. Fish. Manage.* **23**(2): 362–375. doi:10.1577/1548-8675(2003)023<0362:IOFATO>2.0.CO;2.
- Courter, I.L., Garrison, T.M., Kock, T.J., Perry, R.W., Child, D.B., and Hubble, J.D. 2016. Benefits of prescribed flows for salmon smolt survival enhancement vary longitudinally in a highly managed river system. *River Res. Appl.* **32**(10): 1999–2008. doi:10.1002/rra.3066.
- Coutant, C.C., and Whitney, R.R. 2000. Fish behavior in relation to passage through hydropower turbines: a review. *Trans. Am. Fish. Soc.* **129**(2): 351–380. doi:10.1577/1548-8659(2000)129<0351:FBIRTPM>2.0.CO;2.
- Denwood, M.J. 2016. runjags: an R package providing interface utilities, model templates, parallel computing methods and additional distributions for MCMC models in JAGS. *J. Stat. Softw.* **71**(9): 1–25. doi:10.18637/jss.v071.i09.
- Ferrari, M.C., Ranåker, L., Weinersmith, K.L., Young, M.J., Sih, A., and Conrad, J.L. 2013. Effects of turbidity and an invasive waterweed on predation by introduced largemouth bass. *Environ. Biol. Fishes.* **97**(1): 79–90. doi:10.1007/s10641-013-0125-7.
- Gelman, A., Carlin, J.B., Stern, H.S., Dunson, D.B., Vehtari, A., and Rubin, D.B. 2013. Bayesian data analysis. CRC Press, Boca Raton, Fla.
- Gibson, A.J.F., Halfyard, E.A., Bradford, R.G., Stokesbury, M.J., and Redden, A.M. 2015. Effects of predation on telemetry-based survival estimates: insights from a study on endangered Atlantic salmon smolts. *Can. J. Fish. Aquat. Sci.* **72**(5): 728–741. doi:10.1139/cjfas-2014-0245.
- Grossman, G.D. 2016. Predation on fishes in the Sacramento–San Joaquin Delta: current knowledge and future directions [online]. San Francisco Estuary and Watershed Science, **14**(2). Available from <http://escholarship.org/uc/item/9rw9b5tj> [accessed 12 July 2017].
- Halfyard, E.A., Gibson, A.J.F., Stokesbury, M.J., Ruzzante, D.E., and Whoriskey, F.G. 2013. Correlates of estuarine survival of Atlantic salmon

- postsmolts from the Southern Upland, Nova Scotia, Canada. *Can. J. Fish. Aquat. Sci.* **70**(3): 452–460. doi:10.1139/cjfas-2012-0287.
- Healey, M., Goodwin, P., Dettinger, M., and Norgaard, R. 2016. The State of Bay-Delta Science 2016: An Introduction [online]. San Francisco Estuary and Watershed Science, **14**(2). Available from <http://escholarship.org/uc/item/9k43h252>. [accessed 12 July 2017]. doi:10.15447/sfew.2016v14iss2art5.
- King, R., Morgan, B., Gimenez, O., and Brooks, S. 2010. Bayesian analysis for population ecology. CRC Press, Boca Raton, Fla.
- Kjelson, M.A., and Brandes, P.L. 1989. The use of smolt survival estimates to quantify the effects of habitat changes on salmonid stocks in the Sacramento–San Joaquin rivers, California. In *Proceedings of the National Workshop on Effects of Habitat Alteration on Salmonid Stocks*, Nanaimo, B.C., 6–8 May 1987. Canadian Special Publication of Fisheries and Aquatic Sciences 105, Department of Fisheries and Oceans, Ottawa, Ont., Canada. pp. 100–115.
- Kjelson, M.A., Raquel, P.F., and Fisher, F.W. 1982. Life history of fall-run juvenile Chinook salmon, *Oncorhynchus tshawytscha*, in the Sacramento–San Joaquin Estuary, California. In *Estuarine Comparisons*. Edited by V.S. Kennedy. Academic Press, New York. pp. 393–411.
- Link, W.A., and Barker, R.J. 2010. Bayesian inference: with ecological applications. Academic Press, San Diego, Calif.
- Lund, B., Brandt, S., Collier, T., Atwater, B., Canuel, E., Fernando, H.J.S., Meyer, J., Norgaard, R., Resh, V., Wiens, J., and Zedler, J. 2015. Flows and fishes in the Sacramento–San Joaquin Delta: Research needs in support of adaptive management [online]. Delta Stewardship Council, Sacramento, Calif. Available from <http://deltacouncil.ca.gov/sites/default/files/2015/09/2015-9-29-15-0929-Final-Fishes-and-Flows-in-the-Delta.pdf> [accessed 12 July 2017].
- Michel, C.J., Ammann, A.J., Lindley, S.T., Sandstrom, P.T., Chapman, E.D., Thomas, M.J., Singer, G.P., Klimley, A.P., and MacFarlane, R.B. 2015. Chinook salmon outmigration survival in wet and dry years in California's Sacramento River. *Can. J. Fish. Aquat. Sci.* **72**(11): 1749–1759. doi:10.1139/cjfas-2014-0528.
- Monnahan, C.C., Thorson, J.T., and Branch, T.A. 2017. Faster estimation of Bayesian models in ecology using Hamiltonian Monte Carlo. *Methods Ecol. Evol.* **8**(3): 339–348. doi:10.1111/2041-210X.12681.
- Moser, M.L., Olson, A.F., and Quinn, T.P. 1991. Riverine and estuarine migratory behavior of coho salmon (*Oncorhynchus kisutch*) smolts. *Can. J. Fish. Aquat. Sci.* **48**(9): 1670–1678. doi:10.1139/f91-198.
- Mount, J., Bennett, W., Durand, J., Fleenor, W., Hanak, E., Lund, J., and Moyle, P. 2012. Aquatic ecosystem stressors in the Sacramento–San Joaquin Delta [online]. Public Policy Institute of California, San Francisco, Calif. Available from http://www.ppic.org/content/pubs/report/R_612JMR.pdf [accessed 12 July 2017].
- Muthukumarana, S., Schwarz, C.J., and Swartz, T.B. 2008. Bayesian analysis of mark-recapture data with travel time-dependent survival probabilities. *Can. J. Stat.* **36**(1): 5–21. doi:10.1002/cjs.5550360103.
- Newman, K.B. 2003. Modelling paired release-recovery data in the presence of survival and capture heterogeneity with application to marked juvenile salmon. *Stat. Modell.* **3**(3): 157–177. doi:10.1191/1471082X03st055oa.
- Newman, K.B., and Brandes, P.L. 2010. Hierarchical modeling of juvenile Chinook salmon survival as a function of Sacramento–San Joaquin Delta water exports. *N. Am. J. Fish. Manage.* **30**(1): 157–169. doi:10.1577/M07-188.1.
- Newman, K.B., and Rice, J. 2002. Modeling the survival of Chinook salmon smolts outmigrating through the lower Sacramento River system. *J. Am. Stat. Assoc.* **97**(460): 983–993. doi:10.1198/016214502388618771.
- Papaspiliopoulos, O., Roberts, G.O., and Skögl, M. 2007. A general framework for the parametrization of hierarchical models. *Stat. Sci.* **22**(1): 59–73. doi:10.1214/088342307000000014.
- Perry, R.W. 2010. Survival and migration dynamics of juvenile Chinook salmon (*Oncorhynchus tshawytscha*) in the Sacramento–San Joaquin River Delta. Ph.D. dissertation, School of Aquatic and Fishery Sciences, University of Washington, Seattle, Wash.
- Perry, R.W., Skalski, J.R., Brandes, P.L., Sandstrom, P.T., Klimley, A.P., Ammann, A., and MacFarlane, B. 2010. Estimating survival and migration route probabilities of juvenile Chinook salmon in the Sacramento–San Joaquin River Delta. *N. Am. J. Fish. Manage.* **30**(1): 142–156. doi:10.1577/M08-200.1.
- Perry, R.W., Romine, J.G., Brewer, S.J., LaCivita, P.E., Brostoff, W.N., and Chapman, E.D. 2012. Survival and migration route probabilities of juvenile Chinook salmon in the Sacramento–San Joaquin River Delta during the winter of 2009–10. US Geological Survey Open File Report No. 2012-1200 [online]. Available from <https://pubs.usgs.gov/of/2012/1200/> [accessed 12 July 2017].
- Perry, R.W., Brandes, P.L., Burau, J.R., Klimley, A.P., MacFarlane, B., Michel, C., and Skalski, J.R. 2013. Sensitivity of survival to migration routes used by juvenile Chinook salmon to negotiate the Sacramento–San Joaquin River Delta. *Environ. Biol. Fishes.* **96**(2–3): 381–392. doi:10.1007/s10641-012-9984-6.
- Perry, R.W., Brandes, P.L., Burau, J.R., Sandstrom, P.T., and Skalski, J.R. 2015. Effect of tides, river flow, and gate operations on entrainment of juvenile salmon into the Interior Sacramento–San Joaquin River delta. *Trans. Am. Fish. Soc.* **144**(3): 445–455. doi:10.1080/00028487.2014.1001038.
- Perry, R.W., Buchanan, R.A., Brandes, P.L., Burau, J.R., and Israel, J.A. 2016. Anadromous salmonids in the Delta: new science 2006–2016 [online]. San Francisco Estuary and Watershed Science, **14**(2). Available from <http://escholarship.org/uc/item/27f0s5kh> [accessed 12 July 2017]. doi:10.15447/sfew.2016v14iss2art7.
- R Core Team. 2015. R: a language and environment for statistical computing [online]. R Foundation for Statistical Computing, Vienna, Austria. Available from <https://www.R-project.org/> [accessed 20 October 2017].
- Raymond, H.L. 1988. Effects of hydroelectric development and fisheries enhancement on spring and summer chinook salmon and steelhead in the Columbia River basin. *N. Am. J. Fish. Manage.* **8**(1): 1–24. doi:10.1577/1548-8675(1988)008<0001:EOHDAF>2.3.CO;2.
- Romine, J.G., Perry, R.W., Pope, A.C., Stumpner, P., Liedtke, T.L., Kumagai, K.K., and Reeves, R.L. 2017. Evaluation of a floating fish guidance structure at a hydrodynamically complex river junction in the Sacramento–San Joaquin River Delta, California, USA. *Mar. Freshw. Res.* **68**(5): 878–888. doi:10.1071/MF15285.
- Sabal, M., Hayes, S., Merz, J., and Setka, J. 2016. Habitat alterations and a nonnative predator, the Striped Bass, increase native Chinook Salmon mortality in the Central Valley, California. *N. Am. J. Fish. Manage.* **36**(2): 309–320. doi:10.1080/02755947.2015.1121938.
- Satterthwaite, W.H., Carlson, S.M., Allen-Moran, S.D., Vincenzi, S., Bograd, S.J., and Wells, B.K. 2014. Match-mismatch dynamics and the relationship between ocean-entry timing and relative ocean recoveries of Central Valley fall run Chinook salmon. *Mar. Ecol. Prog. Ser.* **511**: 237–248. doi:10.3354/meps10934.
- Skalski, J.R., Townsend, R., Lady, J., Giorgi, A.E., Stevenson, J.R., and McDonald, R.D. 2002. Estimating route-specific passage and survival probabilities at a hydroelectric project from smolt radiotelemetry studies. *Can. J. Fish. Aquat. Sci.* **59**(8): 1385–1393. doi:10.1139/f02-094.
- Smith, S.G., Muir, W.D., Williams, J.G., and Skalski, J.R. 2002. Factors associated with travel time and survival of migrant yearling Chinook salmon and steelhead in the lower Snake River. *N. Am. J. Fish. Manage.* **22**(2): 385–405. doi:10.1577/1548-8675(2002)022<0385:FAWTTA>2.0.CO;2.
- Smith, S.G., Muir, W.D., Hockersmith, E.E., Zabel, R.W., Graves, R.J., Ross, C.V., Connor, W.P., and Arnsberg, B.D. 2003. Influence of river conditions on survival and travel time of Snake River subyearling fall Chinook salmon. *N. Am. J. Fish. Manage.* **23**(3): 939–961. doi:10.1577/M02-039.
- Sparling, Y.H., Younes, N., Lachin, J.M., and Bautista, O.M. 2006. Parametric survival models for interval-censored data with time-dependent covariates. *Biostatistics*, **7**(4): 599–614. doi:10.1093/biostatistics/kxj028.
- Stich, D.S., Bailey, M.M., Holbrook, C.M., Kinnison, M.T., and Zydlewski, J.D. 2015. Catchment-wide survival of wild- and hatchery-reared Atlantic salmon smolts in a changing system. *Can. J. Fish. Aquat. Sci.* **72**(9): 1352–1365. doi:10.1139/cjfas-2014-0573.
- Thorstad, E.B., Whoriskey, F., Uglem, I., Moore, A., Rikardsen, A.H., and Finstad, B. 2012. A critical life stage of the Atlantic salmon *Salmo salar*: behaviour and survival during the smolt and initial post-smolt migration. *J. Fish Biol.* **81**(2): 500–542. doi:10.1111/j.1095-8649.2012.03370.x. PMID:22803722.
- Tiffan, K.F., Kock, T.J., Haskell, C.A., Connor, W.P., and Steinhilber, R.K. 2009. Water velocity, turbulence, and migration rate of subyearling fall Chinook salmon in the free-flowing and impounded Snake River. *Trans. Am. Fish. Soc.* **138**(2): 373–384. doi:10.1577/T08-051.1.
- Vogel, J.L., and Beauchamp, D.A. 1999. Effects of light, prey size, and turbidity on reaction distances of lake trout (*Salvelinus namaycush*) to salmonid prey. *Can. J. Fish. Aquat. Sci.* **56**(7): 1293–1297. doi:10.1139/f99-071.
- Ward, J.H., Jr. 1963. Hierarchical grouping to optimize an objective function. *J. Am. Stat. Assoc.* **58**(301): 236–244. doi:10.1080/01621459.1963.10500845.
- White, G.C., and Burnham, K.P. 1999. Program MARK: survival estimation from populations of marked animals. *Bird Study*, **46**(s1): S120–S139. doi:10.1080/00063599909477239.
- Zabel, R.W. 2002. Using “travel time” data to characterize the behavior of migrating animals. *Am. Nat.* **159**(4): 372–387. doi:10.1086/338993. PMID:18707422.
- Zabel, R.W., and Anderson, J.J. 1997. A model of the travel time of migrating juvenile salmon, with an application to Snake River spring chinook salmon. *N. Am. J. Fish. Manage.* **17**(1): 93–100. doi:10.1577/1548-8675(1997)017<0093:AMOTT>2.3.CO;2.
- Zabel, R.W., Burke, B.J., Moser, M.L., and Caudill, C.C. 2014. Modeling temporal phenomena in variable environments with parametric models: an application to migrating salmon. *Ecol. Modell.* **273**: 23–30. doi:10.1016/j.ecolmodel.2013.10.020.